



**ADDIS ABABA UNIVERSITY**

**ADDIS ABABA INSTITUTE OF TECHNOLOGY**

**SCHOOL OF CIVIL AND ENVIRONMENTAL ENGINEERING**

**Assessment of Shear Capacity of Reinforced Concrete Beam  
Sections Using Modified Compression Field Theory**

Thesis Submitted to Postgraduate Studies in Partial Fulfillment  
of the Requirements for the Degree of Master of Science  
in Structural Engineering

By Tizazu Geremew

October, 2020  
Addis Ababa, Ethiopia

The undersigned have examined the thesis entitled ‘**Assessment of Shear Capacity of Reinforced Concrete Beam Sections Using Modified Compression Field Theory**’ presented by **Tizazu Geremew** , a candidate for the degree of **Master of Science** and hereby certify that it is worthy of acceptance.

Dr Esayas Gebreyohannes

Advisor

Signature

Date

Dr. Bedilu Habte

Internal Examiner

Signature

Date

Dr. Adil Zekaria

External Examiner

Signature

Date

Chair person

Signature

Date

## **UNDERTAKING**

I certify that research work titled “**Assessment of Shear Capacity of Reinforced Concrete Beam Sections Using Modified Compression Field Theory**” is my own work. The work has not been presented elsewhere for assessment. Where material has been used from other sources it has been properly acknowledged.

**Tizazu Geremew**

## **ABSTRACT**

The behavior and design of reinforced concrete members subjected to shear remain an area of much concern and investigation. This is particularly due to the less knowledge on shear resistance mechanism of RC structures in one extent and also shear is affected by a number of factors which are not interdependent to each other. In addition to this many structures were failed due to shear throughout the world. Several researches and proposals were developed for predicting the shear strength of beams in different times by different scholars throughout the engineering world. Most of them were empirical formulations designed to fit the limited set of experimental results for shear.

Also different countries adopted design codes based on test results and these codes are continuously changing which necessitates a method that performs further checks on the performance of structures which were designed and constructed based on the previous codes which became outdated. Due to this it is very essential to adopt a theory which forms its basis mainly on the mechanics of members and which gets verified by experimental findings. One of such method is modified compression field theory which is an extension of the compression field theory. It is an analytical model that is largely based on experimental results from University of Toronto by Vecchio and Collins.

Particularly, to Ethiopia, where a new code is adopted it is very important to have a tool to assess the performance of structures subjected to shear. So this study presents a tool that can perform shear capacity check based on MCFT using Microsoft visual basic mathematical programming language. The results from the tool are compared with the available codes of ACI and Euro code. With this regard, the shear capacities of all sections obtained by modified compression field theory is greater than that of both the Euro code values and the ACI values as also indicated in previous works of Surafel Tsegaye. Also, the Euro code values are the least values among the three because in Euro code the shear is assumed to be resisted by the shear reinforcements only. On the otherhand for continuous beam sections relatively consistent results were obtained.

**Key words:-** Shear, Shear capacity, Modified Compression Field Theory, Concrete

## **ACKNOWLEDGMENTS**

First of all, I would like to thank God for the time and the patience He gave me for completing this thesis.

Next, I would like to thank my advisor, Dr.-Esayas Gebreyohannes who had given me his full support in guiding me with motivating suggestions and encouragement to go ahead in all the time of the thesis work.

I also extend my gratitude towards my friends for their support and help. In particular, I am very much thankful of Mr. Mikiyas Dasa who helped me in providing information and idea in the development of the thesis document.

Special thanks for Addis Ababa Institute of Technology and Ethiopian Road Authority for academic sponsor.

# TABLE OF CONTENTS

<b>ABSTRACT</b> .....	<b>I</b>
<b>ACKNOWLEDGMENTS</b> .....	<b>II</b>
<b>LIST OF TABLES</b> .....	<b>VI</b>
<b>LIST OF FIGURES</b> .....	<b>VII</b>
<b>LIST OF ABBREVIATION</b> .....	<b>VIII</b>
<b>CHAPTER 1 INTRODUCTION</b> .....	<b>1</b>
1.1 Background information .....	1
1.2 Statements of the Problem.....	2
1.3 Aim of the Study .....	2
1.3.1 Specific Objectives .....	2
1.4 Scope and Limitation .....	3
1.5 Outline of the Study .....	3
1.6 Methodology .....	3
<b>CHAPTER 2 LITERATURE REVIEW</b> .....	<b>4</b>
2.1 Cracking in Concrete.....	4
2.2 Mechanism of Shear Transfer after Diagonal Cracking.....	6
2.3 Shear Models.....	8
2.3.1 The 45 Degree Truss Model .....	8
2.3.2 Variable-Angle Truss Model .....	9
2.3.3 Compression Field Theory and Modified Compression Field Theory .....	9
2.3.4 Modified Compression Field Theory.....	10
2.3.5 Disturbed Stress Field Theory .....	11
2.4 Codes of Practice.....	12
2.4.1 EC2 .....	12
2.4.2 ACI.....	13
2.4.3 JSCE (1986).....	13

<b>CHAPTER 3</b>	<b>MODIFIED COMPRESSION FIELD THEORY .....</b>	<b>15</b>
3.1	Compatibility.....	15
3.2	Equilibrium Conditions .....	17
3.3	Constitutive Relations of Concrete .....	18
3.4	Important Aspects of the MCFT .....	21
3.4.1	Reinforcement average response .....	21
3.4.2	Concrete tensile stress response ( $f_1$ ) .....	21
3.4.3	Concrete compressive stress response ( $f_2$ ).....	21
3.4.4	Crack width ( $\omega$ ).....	21
3.4.5	Shear on the crack ( $v_{ci}$ ) .....	22
3.4.6	Local reinforcement stress at a crack ( $f_{scrx}$ , $f_{sry}$ ).....	22
3.4.7	The Crack Check.....	22
3.5	Sectional-Based Analysis of Concrete Structures .....	23
3.5.1	Types of Sectional Analyses .....	27
3.5.2	Secant Stiffness Formulation .....	28
3.5.3	The Longitudinal Stiffness Method .....	30
3.6	Solving problems with the MCFT.....	31
3.6.1	Response Procedure using MCFT .....	32
3.6.2	Design Procedure Using MCFT.....	38
<b>CHAPTER 4</b>	<b>ANALYSIS AND ALGORITHMS DEVELOPMENT .....</b>	<b>40</b>
4.1	Algorithms Development .....	40
4.2	Analysis.....	42
4.2.1	Shear Design Procedure Using Euro Code .....	43
4.2.2	Design Procedure Using ACI Code .....	53
4.2.3	Shear Strength Calculation Using MCFT.....	60
<b>CHAPTER 5</b>	<b>RESULT AND DISCUSSION .....</b>	<b>64</b>
<b>CHAPTER 6</b>	<b>CONCLUSIONS AND RECOMMENDATIONS .....</b>	<b>67</b>

6.1	Conclusions .....	67
6.2	Recommendations .....	67
	<b>REFERENCE .....</b>	<b>69</b>
	<b>APPENDIX A:.....</b>	<b>71</b>



## **LIST OF TABLES**

Table 4-1 Summary of shear results of Euro code shear design procedure.....	52
Table 4-2 Summary of the shear design results of ACI shear design procedure .....	60
Table 4-3 Summary of shear design results .....	60
Table 5-1 Comparison of shear capacity of sections according to Euro Code, ACI and MCFT..	64

## LIST OF FIGURES

Figure 1.1 Typical shear failure mechanisms of reinforced concrete (Kraczla, 2016).....	2
Figure 2.1 Stress in a segment of concrete; a) a beam subjected to four point bending b) and c) shear stresses in a concrete segment; d) stress resolution; e) stresses in the principal directions ..	5
Figure 2.2 Principal stresses in individual locations a) beam with segments' locations; b) segment A principal stress; c) segment B; d) segment C (Kraczla, 2016) .....	6
Figure 2.3 Stress field before and after cracking in a reinforced element (Kraczla, 2016) .....	7
Figure 2.4 Crack surface in cracked concrete .....	8
Figure 2.5 (a) Ritter's original truss analogy for shear; and (b) concrete stresses.....	9
Figure 3.1 Average Concrete Strains (Güner, 2008) .....	15
Figure 3.2 Mohr's Circle of average strain (Güner, 2008) .....	16
Figure 3.3 Free Body Diagram of a Reinforced Concrete Element Showing Average stresses...	17
Figure 3.4 Two dimensional crack check (Bentz, 2000) .....	23
Figure 3.5 Longitudinal Strain Distribution.....	25
Figure 3.6 Input Parameters for Sectional Analysis (Güner, 2008).....	26
Figure 3.7 Longitudinal and Shear Strain Distribution across Cross Section Depth.....	27
Figure 3.8 Shear flow and shear strain based on Vecchio's rigorous and approximate approaches (CHAN, 2008).....	29
Figure 3.9 Shear stress calculation (Bentz, 2000).....	30
Figure 3.10 Internals of shear stress calculation.....	31
Figure 4.1 Flow chart.....	42
Figure 4.2 Beam sections used for shear capacity comparison .....	43
Figure 4.3 Main window showing menu strips.....	61
Figure 4.4 Main window showing material properties .....	62
Figure 4.5 Main window showing section properties.....	62
Figure 4.6 Main window showing design inputs .....	63
Figure 5.1 Comparison of MCFT and Euro code .....	65
Figure 5.2 Comparison of ACI and MCFT.....	65

## LIST OF ABBREVIATION

CFT= compression field theory

C# = C sharp

MCFT= modified compression field theory

a=maximum aggregate size

$A_c$  = concrete area

$A_s$ = area of steel reinforcement

$A_{s1}$ = area of tensile reinforcement in beam section

$A_v$ = area of shear reinforcement

$A_{v,min}$  = minimum shear reinforcement area

$b_w$ = width of the beam

C = compressive force

D = the vertical components of the diagonal compression force

d= effective depth

$E_c$  = modulus of elastic of concrete (initial tangent stiffness)

$E_s$ = modulus of elasticity of reinforcement

$\epsilon_1$ = principal tensile strain in concrete (positive quantity)

$\epsilon_2$ = principal compressive strain in concrete (negative quantity)

$\epsilon'_c$ = strain in concrete cylinder strength at peak stress (negative quantity)

$\epsilon_{Cr}$ = strain in concrete at cracking

$\epsilon_{cx}$ = strain in concrete in x-direction

$\epsilon_{cy}$  = strain in concrete in y-direction

$\epsilon_{sx}$  = strain in reinforcement steel in x-direction

$\epsilon_{sy}$  = strain in reinforcement steel in y-direction

$\epsilon_{\text{bot}}$  = bottom fiber strain in beam section

$\epsilon_{\text{top}}$  = top fiber strain in beam section

$\epsilon_x$  = strain in x-direction

$\epsilon_y$  = strain in y-direction

$\epsilon_{yx}$  = yield strain in x-reinforcement

$\epsilon_{yy}$  = yield strain in y-reinforcement

$f'_c$  = maximum compressive stress observed in cylinder test (negative quantity)

$f_{c1}$  = principal tensile stress in concrete

$f_{c2}$  = principal compressive stress in concrete (negative quantity)

$f_c$  = compressive stress

$f_t$  = tensile stress

$f_1$  = principal stress in orthogonal plane

$f_2$  = principal stress in orthogonal plane

$f_{ct}$  = compressive stress on crack surface (positive quantity)

$f_{cr}$  = stress in concrete at cracking

$f_{cx}$  = stress in concrete in x-direction

$f_{cy}$  = stress in concrete in y-direction

$f_{sx}$  = average stress in x-reinforcement

$f_{sy}$  = average stress in y-reinforcement

$f_{sxcr}$  = stress in x-reinforcement at crack location

$f_{syncr}$  = stress in y-reinforcement at crack location

$f_x$  = stress applied to element in x-direction

$f_y$  = stress applied to element in y-direction

$f_{yx}$  = yield stress in x-reinforcement

$f_{yy}$  = yield stress in y-reinforcement

$h$  = depth of a concrete layer

$H$  = overall depth of beam cross-section

$I$  = the second moment of area

$M$  = bending moment

$N$  = axial Force

$Q$  = the first moment of area about the neutral axis

$s$  = spacing of shear reinforcement measured along the longitudinal axis of the structural member.

$S_{\max}$  = maximum spacing of shear reinforcement

$S_{\theta}$  = spacing of cracks inclined at  $\theta$

$s_{mx}$  = average spacing of cracks perpendicular to x-reinforcement

$s_{my}$  = average spacing of cracks perpendicular to y-reinforcement

$T$  = tensile force

DSFM = Disturbed stress field model

RCFT = Refined compression field theory

RA-STM = Rotating angle softened truss model

# Chapter 1 INTRODUCTION

## 1.1 Background information

In many designs, the governing aspect dictating the section dimensions is generally not the shear phenomenon. It is however well known that a shear failure requires special attention. It is a failure mechanism, which comes from a low degree of redundancy in beam elements, is sudden and therefore a minimum amount of shear reinforcement should be provided. An element subjected to a certain load can display two types of cracking, namely flexural cracking and shear tension cracking. The cracking occurs when the principal tensile stresses in the considered section exceed the tensile strength of the concrete. The principal tensile stresses act perpendicular/normal to the principal compressive stresses, thus these paths can be a representation of the directions of crack development. Depending on a crack type and aspects contributing the cracks development (a region of crack occurrence, a cross section type and geometry etc.), two main failure mechanisms can be distinguished. The diagonal tension shear failure is depicted in Figure 1-1a which is originated from the flexural cracks nearest the support (where the shear force is the greatest). The flexural cracks develop into the inclined shear-flexure crack and propagate further till the failure mechanism occurs. As a vast majority of beam elements fail in this manner, it is therefore a very common failure mechanism. The second failure mechanism is related to shear tension cracking, hence called the shear tension failure, Figure 1-1b. This is very brittle failure type appears in beams with thin webs in regions where shear force is large compared to bending moment (e.g. a point of contra flexure or in a vicinity of a support).

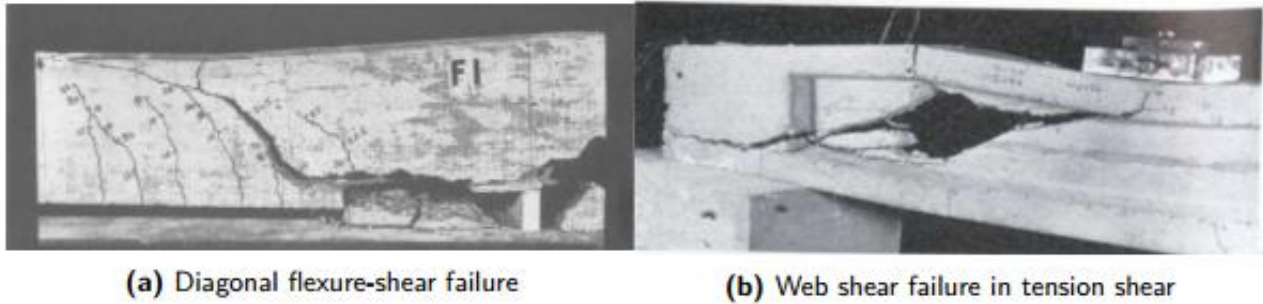


**Figure 1.1 Typical shear failure mechanisms of reinforced concrete** (Kraczla, November 14, 2016)

## **1.2 Statements of the Problem**

Very extensive and important experimental work was done both in university of Toronto and University of Houston mainly led by Vecchio and Collins (1986) and Belabri and Hsu for the investigation of shear response of structures at element level respectively. The findings were very important to the shear science, but most codes such as Euro code still adopt truss analogy both for design and analysis of structures for shear. The behavior of concrete before cracking and post cracking is not incorporated in the shear capacity formulation in Euro code. So it is very essential to investigate and evaluate the limitations in the codes by comparing with MCFT and develop a code which can simplify the calculation of shear capacity.

## **1.3 Aim of the Study**

The main objective is to compare the shear capacity of reinforced concrete beams obtained by Euro code and ACI code with MCFT method and to develop a code that can calculate the shear capacity of RC beam using MCFT.

### **1.3.1 Specific Objectives**

- To assess the shear resistance of reinforced concrete beams using modified compression field theory using multi-layer sectional analysis.
- To indicate the state of art of shear design and analysis models.

- To initiate future researchers to give attention to current shear design models and investigate the gaps in codes specially the Euro code and ACI code.
- To develop a simplified computer code on Microsoft Visual Basic 2015.

## **1.4 Scope and Limitation**

This thesis is limited to the determination of shear resistance of reinforced concrete structures of rectangular section using MCFT based on shear stress based multi-layer sectional analysis in which shear flow is assumed to be uniform.

## **1.5 Outline of the Study**

This study is composed of seven chapters. The first chapter presents the objective of the study, statements of the problem. Methodology and background information about the study topic. The second chapter presents the literature review on Modified compression field theory. In the third chapter the concept of MCFT is presented in detail. The basic principles of MCFT are discussed and the formulations of MCFT based on different sectional analysis are also shown. In the fourth chapter the algorithm is developed and analysis of different beam section is performed using the programme developed and the available design codes of ACI and Euro code. In the fifth chapter the results were compared and the difference are discussed. The sixth chapter presents conclusion and recommendations based on the findings.

## **1.6 Methodology**

Different sections of reinforced concrete beam are designed for shear and analyzed using three approaches. Two of these approaches are Euro code and ACI code. On the other hand window form application was developed based on a computer program on Microsoft Visual Studio 2015. The necessary information were inserted in to the program and the shear capacity of the beam sections is calculated.



## **Chapter 2 LITERATURE REVIEW**

In design of structural elements for moment and axial loads, engineers can make use of available general and rational method called the "plane sections" theory. With this method it is possible to predict both the flexural strength and the complete load-deformation response of reinforced concrete elements. The theory has proved its validity and therefore there is little disagreement in different design codes on the design of the flexural strength or the required amount of reinforcement needed to ensure ductile flexural behaviour. In contrast to flexure, there is substantial disagreement on how to design reinforced concrete members to ensure ductile shear behaviour. Over the years different methods have been proposed. Upon the lack of universally agreed model for shear behaviour, codes of practice propose complex, restricted or purely empirical equations for estimation of shear strength. In addition to that they tend to be conservative imposing more severe safety requirements which leads to their inapplicability for evaluation of existing structures (Kraczla, 2016).

Good understanding of shear behaviour of concrete structures is essential to properly design members against shear failure. Therefore, this section will provide a reader with general information about shear. A review of shear design in codes of practice shear models further used in the analytical solution will be introduced and explained.

### **2.1 Cracking in Concrete**

In Figure 2-1 a small segment at the level of neutral axis of a beam subjected to certain loading is illustrated. From the vertical equilibrium, there appear to be two vertical opposite stresses acting on either side of the segment which tend to rotate the segment clockwise. To prevent from this rotation and to obtain the overall equilibrium, two additional balancing stresses are required on horizontal faces of the segment. Such stresses are called the principal stresses and are of great importance as far as cracking is concerned. The principal stresses therefore are defined as the normal stresses on the face oriented in such a way that shear stress vanishes. From 2-1(e), it can be seen that such tensile stresses are a cause of the crack at 45 degrees to the horizontal. It is important to note that cracking occurs when the principal tensile stresses exceed the tensile strength of concrete. For the segments not in line with the neutral axis, additional axial stresses as a result of bending moment should be accounted for.

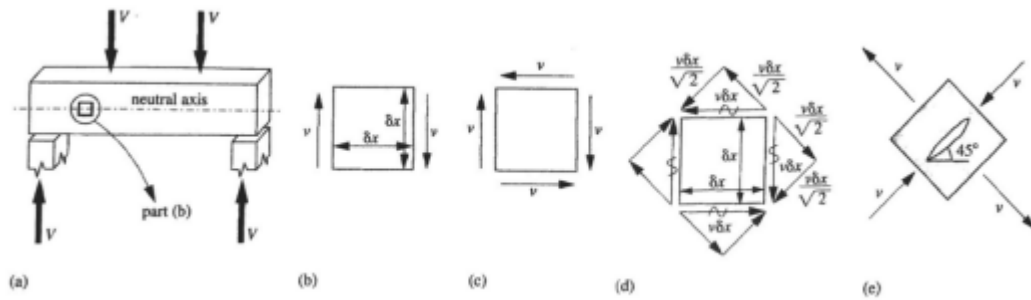


**Figure 2.1 Stress in a segment of concrete; a) a beam subjected to four point bending b) and c) shear stresses in a concrete segment; d) stress resolution; e) stresses in the principal directions**  
 (Kraczla, November 14, 2016)

First type of cracking called web-shear cracking occurs in a section where shear stresses prevail. It is not a very common type of cracking but can appear in sections near a point of contra flexure which is where bending moment is negligible and shear force predominates or in members with thin webs and a limited amount of shear reinforcement (often considered as elements without shear links) such as for example T or I girders. The distinctive features of this type of cracking are cracks propagating from the level in a close proximity of the neutral axis. Another type of cracking is called flexural cracking. For the segment located at the bottom of a member, shear stress in an extreme bottom fibre equal to zero while bending normal stresses have the maximum value. As a result, the principal stresses act normal to the vertical plane. It was previously shown that there exist two limits. For the segment at the level of neutral axis (for zero bending stress and the maximum shear stress) crack inclines at the angle of 45 degrees, Figure 2-2(b) while for pure bending stresses and the extreme bottom fibre a crack appears at the angle of 90 degrees. In the segment between the neutral axis and the bottom of the member, a combination of bending and shear stresses is acting on the element and therefore the crack will develop with an inclination of between 45 and 90 degrees, Figure 2-2(d). At any point/segment of a beam, an inclination of principal stresses can be determined through the Mohr's Circle. It can be well represented by means of stress paths through the member, Figure 2-2, where the dashed lines are the trajectories along which cracks will tend to develop. It is clear that the inclination of the crack will decrease towards the neutral axis as the shear stress become larger and the axial stresses from bending approach zero. The stress paths however are only an indication and it is by no means in

agreement with the crack patterns developed in practice. Such a model does not account for many aspects such as for example redistribution of the shear stresses which occurs when cracks are formed (Kraczla, 2016).

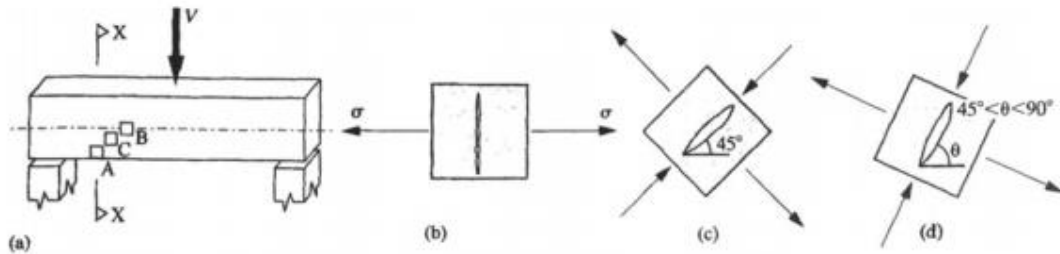


**Figure 2.2 Principal stresses in individual locations a) beam with segments' locations; b) segment A principal stress; c) segment B; d) segment C (Kraczla, 2016)**

## 2.2 Mechanism of Shear Transfer after Diagonal Cracking

Prior to cracking of concrete, shear in the beam's web is carried by diagonal compressive stresses at a certain angle of inclination complemented with perpendicular to them diagonal tensile stresses. The steel bars (if present) have a negligible effect on the behaviour of reinforced concrete element. For such a concrete element (without inclusion of steel bars), the principal stresses coincide with the applied principal stresses. Once the tensile strength of concrete is reached, cracks form and the ability of concrete to transmit principal tensile stresses is substantially reduced (for the cracks width greater than 0.05 mm significant transmission does not occur) and unless a member is sufficiently reinforced, failure may develop. The purpose of such reinforcement is therefore to carry shear. In the case of an element reinforced with a different amount of reinforcement in two directions, the principal coordinate of the concrete element will deviate from the applied principal stresses coordinate of the RC element. The deviation will increase under the shear stress increase until the maximum angle is reached which relates to the yielding of the steel.

Before cracking the principal stresses in both compression and tension are equally engaged in resisting the shear. After cracking however, under the assumption that tensile stresses in concrete decline to zero, the concrete diagonals have to take over the part previously carried

by principal tensile stresses, thus principal compressive stresses double in the value. If the beam is appropriately reinforced, the imbalance is redistributed with longitudinal reinforcement in tension balancing the longitudinal component of the diagonal compression and the web reinforcement balancing the transverse component of the diagonal compression.

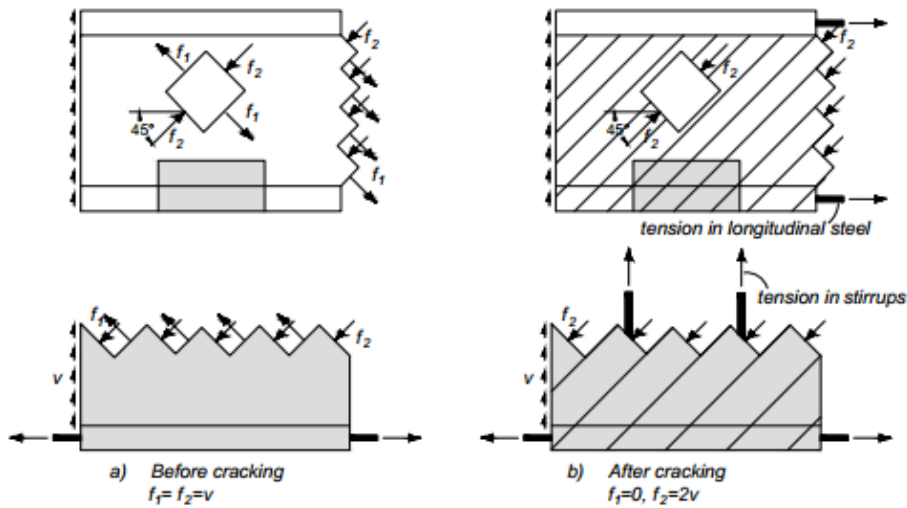


**Figure 2.3** Stress field before and after cracking in a reinforced element (Kraczla, November 14, 2016)

In normal strength concrete, the strength of aggregates is typically higher than the strength of harden cement paste. In the system consisting of the aggregate particles and the matrix, the interface between cement and aggregate (the interfacial transition zone of high porosity) is normally regarded as the weakest link. Because of this, the cracks cross the cement paste, but instead of intersecting further the aggregate particles, the cracks propagate along the edges of the particles creating a rough surface, Figure 2.4. Such protruding aggregates, by means of interlocking one another, generate shear stresses when the relative tangential displacement occurs. This is however only true for regular or low strength concrete. The capacity of aggregate interlock is reduced for concretes with lightweight aggregate and high strength concrete. In the lightweight concrete, as the result of the low strength of aggregate, the crack runs through the particles. Similarly in the latter case, due to the high strength of concrete, the crack proceeds through the matrix as well as the aggregate particles.

Another load carrying mechanism is dowel action of longitudinal reinforcement. It is defined as an ability of reinforcing bars to transfer forces in the direction perpendicular to their axes.

The dowel action occurs upon a crack surface slip which is counteracted by crossed reinforcement. Lastly, the shear can be carried in the uncracked compression zone of a member (**Kraczla, 2016**).

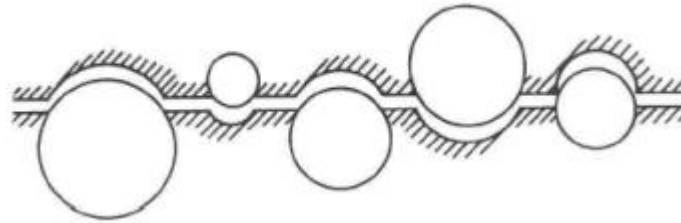


**Figure 2.4 Crack surface in cracked concrete**

## **2.3 Shear Models**

Over the years, a variety of methods have been proposed for predicting the effects of and interactions between the parameters that affect shear capacity, but as yet no unified approach for calculating the shear capacity of reinforced concrete elements has been generally accepted. In the transition from one model to the other there are so many modifications are seen and these improves the knowledge about shear.

### **2.3.1 The 45 Degree Truss Model**

The first truss model with parallel chords was proposed by Ritter. The truss is composed of diagonal compressive struts inclined at the angle of 45 degrees, the transverse tension ties, the top compression chord and bottom tension chord. Later in 1902, the model with discrete diagonal compressive struts was undermined by Mörsh who claimed that the diagonal compression is transferred through a continuous field resisting shear. The 45-degree model comprises of three assumptions: the tensile stresses in the cracked concrete are neglected; the diagonal compression stress coincides with the crack angle and after cracking the angle remains at 45 degrees; the contribution of the top and bottom chords in resisting shear is neglected and shear stresses are uniformly distributed over an effective shear area (**Kraczla, 2016**).

This model (Figure. 2.5) assumes that after cracking, the shear is resisted only by a combination of diagonal compressive stresses  $f_2$  (struts) in the concrete, and a network of

longitudinal and transverse ties, representing the action of the reinforcement (longitudinal bars and stirrups). The  $45^\circ$ -truss model is very conservative in terms of shear strength, because in the members containing usual amounts of stirrups the inclined cracks generally form at a much smaller angle; hence, more transverse reinforcement across an inclined crack is mobilized than in the case of  $45^\circ$  inclination. On the contrary, whenever small amounts of stirrups are provided, stirrup contribution should be neglected, rather than the tensile strength of concrete, whose contribution can be far from negligible (María, 2012).

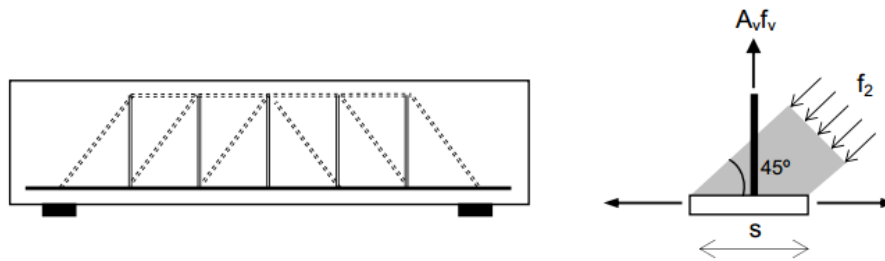


**Figure 2.5 (a) Ritter's original truss analogy for shear; and (b) concrete stresses**

During the 1970s and 1980s, several European researchers focused their attention on the fact that according to the experimental and theoretical findings  $\theta$  is not close to  $45^\circ$ . Hence, an appropriate value of  $\theta$  had to be introduced, contrary to the traditional approach. Models based on the theory of plasticity were developed, in order to allow the designer to select the value of  $\theta$ , but the applicability of this approach was rather controversial, owing to the limited success of plasticity models in representing the actual behavior of concrete (María, 2012).

### 2.3.2 Variable-Angle Truss Model

The variable-angle truss model is based on the same rules as the previous truss model. To account for the fact that the angle  $\theta$  is typically less than  $45^\circ$  for some cases, such as e.g. prestressed members, the model was modified (Kraczla, 2016)

### 2.3.3 Compression Field Theory and Modified Compression Field Theory

#### 2.3.3.1 Compression Field Theory

The Compression Field Theory is a smeared crack continuum mechanics modeling approach in which cracked concrete is treated as a new material with its own stress-strain characteristics. The word smeared in this context refers to the strains expressed in average terms thus the strains are smeared over a base lengths equal at least the crack spacing. The

formulation of the approach comprises of the equilibrium equations of external forces with internal forces, the compatibility equations relating strains in the reinforcement and strains in the concrete and lastly the constitutive relationships linking the average strains and average stresses for the reinforcement and concrete. The equilibrium conditions result from balancing the applied external forces on a RC element and stresses arose in the concrete and the reinforcing steel (Kraczla, 2016).

#### **2.3.4 Modified Compression Field Theory**

The compression field theory assumes that after concrete has cracked, the principal tensile stress is equal to zero. For this reason, CFT overestimates deformations and provides conservative results. In reality, which was found by Vecchio and Collins in the tests on RC panels subjected to pure shear, the residual tensile stresses exist in the concrete between two adjacent cracks which in turn can significantly contribute and increase the ability of concrete to resist the shear. It essentially means that shear after cracking is not carried solely by reinforcement but instead by a combination of the concrete and steel contributions (concrete stiffening) (Kraczla, 2016).

To account for this, the Modified Compression Field Theory was developed which explicitly considers a residual post-peak tensile capacity of reinforced concrete. Unlike traditional shear design approaches, in MCFT, the concrete contribution  $V_c$  is not the shear force at diagonal cracking; but is the additional shear force beyond that resisted by yielding stirrups that can be transferred across diagonal cracks by interlock of rough crack surfaces. (Esfandiari, 2009).

The mechanism of the shear transfer in a panel subjected to shear is classified as average stresses between the cracks and local stresses at the crack location. These two sets of stresses are statically equivalent (their resultants are equal). Because of this, the stresses between two sets impart. It means that the loss of tensile stresses in the concrete at the crack location must result in an increase of steel stresses at the crack or, when the reinforcement yielded due to excessive stresses in shear stresses on the crack interface (aggregate interlock) .The effectiveness of such a shear transfer across the crack depends on the crack width (Kraczla, 2016).

#### ***2.3.4.1 Refined Compression Field Theory (RCFT)***

RCFT proposes a stress–strain relationship for the reinforcing bars stiffened by concrete (embedded bar model); the novelty is that the embedded bar stress–strain relationship is obtained imposing equilibrium on the tension stiffening effect; so new formulation for the steel model would no longer be needed (compared with RA-STM) and the crack check can be avoided (compared with MCFT).

Numerical results obtained from RCFT for different tested specimens (Gil-Martín et al. 2009; Palermo et al. 2013) show a better fitting of the experimental results, in particular near the peak point in the shear response curve, where the MCFT significantly deviates from the experimental evidences.

#### ***2.3.4.2 Rotating Angle Softened Truss Model (RA-STM)***

A different procedure to account for tensile stresses in diagonally cracked concrete was developed by Hsu and his colleagues (Belarbi and Hsu 1994, 1995; Pang and Hsu 1995; Hsu 1993). Like the MCFT, the RA-STM assumes that the inclination of the principal stress direction,  $\theta$ , in the cracked concrete coincides with the principal strain direction, and uses average stresses and average strains in postulating equilibrium and compatibility equations.

RA-STM uses a stress-strain relationship for the reinforcement stiffened by concrete (embedded bars) originally proposed by Belarbi and Hsu (1994). They proposed two forms of stress-strain curves: the first is a single curve using the Richard and Abbott (1975) analytical expression, and the second is a bilinear formulation. In the MCFT, a crack check should be performed to ensure that stresses do not exceed the maximum strength allowed at the crack. If the embedded reinforcement stress-strain model is used, then no crack check is necessary.

#### **2.3.5 Disturbed Stress Field Theory**

The Disturbed Stress Field Model (Vecchio, 2000) is an advanced reformulation of the MCFT that was specifically developed to address reduced accuracy encountered in the MCFT under specific circumstances by extending the MCFT in several aspects. Experience with the MCFT for over 20 years has shown that the MCFT underestimates the shear strength and stiffness of panels containing heavy amounts of reinforcement in both directions when subjected to biaxial compression and shear. In addition, the shear strength and stiffness of panels containing light amounts of transverse reinforcement are overestimated by the MCFT.



These inaccuracies were believed to be partly connected to the assumption of the principal stress and strain axes being collinear. Examination of test data revealed that the direction of principal stress lags behind the direction of principal strain in some cases. This observation led to the removal of the restriction found in the MCFT that the principal stress and strain directions must be coincident. This was achieved by the explicit inclusion of crack slip deformations in the compatibility relations of the DSFM. Through the consideration of these crack slip deformations, it also became possible to eliminate the complex crack slip check required by the MCFT. In addition, the DSFM incorporated improved constitutive relations for both concrete and reinforcement (Güner, Serhan, 2008).

## 2.4 Codes of Practice

While flexural design is concerned with ensuring that the two sides of a member can resist the appropriate magnitudes of tensile or compressive longitudinal forces, shear design is intended to ensure that the two sides of the member continue to act as a unit. This involves identifying where shear reinforcement is required to link together the two sides of the member and determining how much of this reinforcement is needed to prevent a premature shear failure. For regions not containing shear reinforcement, a shear failure can occur without warning and typically involves the opening of a major diagonal crack.

### 2.4.1 EC2

The European standard (EN, 2005) uses different models for beams with and without shear reinforcement; the standard relies on both the plasticity of concrete and the variable angle truss analogy. The model has two separate computational routines that depends on  $V_{Ed}$ , the design shear force resulting from external loading and prestressing (if present), and  $V_{Rd,c}$ , the design shear resistance of the concrete member without shear reinforcement (Sas, 2011).

Euro code 2 (1992): The ultimate shear strength of RC members is determined by summing the contribution of the concrete and the web reinforcement.

$$V_c = V_w + V_s \quad (2.1)$$

The transverse reinforcement contribution to the shear is estimated by the truss mechanism term which is given as

$$V_w = \frac{A_{sw} f_{yd} (0.9 * d)}{s} \quad (2.2)$$

**Euro code 2 (pr EN 1992-1-1:2003):** As the controversy on the estimation of shear strength of reinforcement concrete beams with stirrups continued, it was realized that some of the models are too complex to be implemented in a code of practice. This had to be simplified. Euro code 2 (2003) was then released to simplify matters and to be adapted in the Europe. This modified code seeks to solve some of the challenges that practicing engineers confront with regard to previous code. Cladera and Mari (2007) admits that, this code proposes a very simple formulation based on only the truss model with variable inclination angle of struts without any concrete contribution. This code thus over simplifies the equation resulting into the neglect of important key variables.

EC2 requires that a minimum quantity of shear reinforcement be provided in beams such that  $\rho_w * f_y$  is at least equal to  $0.08 \sqrt{f_{ck}}$ , however this minimum shear reinforcement is not required for members such as slabs.

#### 2.4.2 ACI

Traditional American shear design procedures assumed that such failures of members without shear reinforcement would not occur if the calculated shear stress,  $V/(b_w jd)$ , at service loads was less than about  $0.03fc'$ . If the shear stress was higher than this allowable stress, then shear reinforcement (e.g. links) would be added to carry the excess shear. The capacity added by the links was given by the 45° truss model of Ritter and Morsch as  $\rho_w f_s$  where  $f_s$  was the allowable tensile stress in the links. Such shear reinforcement controls the opening of diagonal cracks and permits much higher shear stresses to be resisted. The applied shear resisted by the combined contribution of the shear reinforcement and the concrete.

#### 2.4.3 JSCE (1986)

The Japanese JSCE code (1986) considers the effect of effective depth of member, the percentage longitudinal reinforcement and the concrete compressive strength in its model to estimate the concrete contribution to shear strength of RC members.

$$V_c = 0.9\beta_d\beta_p\beta_0fc^{1/3}b_wd \quad (2.3)$$

The depth factor,  $\beta_d = \left(\frac{100}{d}\right)^{1/4} \leq 1.5$

The percentage reinforcement effect,  $\beta_p = (100\rho)^{1/3} \leq 1.5$

Shear span to effective depth ratio effect,  $\beta_0 = 0.75 + [1.4 / (a / d)]$

The stirrup contribution is derived from the truss mechanism

$$V_s = \frac{A_{sw}}{s} f_{yw} (j_t \cot \theta) \quad (2.4)$$

## Chapter 3 MODIFIED COMPRESSION FIELD THEORY

Modified Compression Field Theory (MCFT) is a smeared rotating approach treating cracked concrete as a new orthotropic material with its own average stress-strain. Different from the fixed crack approach where crack orientation is fixed after first cracking happened, crack orientation in MCFT changes based on the loading intensity. The method is capable for predicting the behavior of two dimensional RC structures with complex geometry under combined shear and normal stress which is a big advantage over standard sectional analysis where normal and shear forces are uncoupled and there is no effect of shear deformation on normal deformation is considered. The method is based on three principles of solid mechanics of the concrete including compatibility, equilibrium, and constitutive relations as well as additional local crack check (Chan, 2008).

### 3.1 Compatibility

There are two key assumptions are common to all CFT models. Firstly, on the average, any deformation experienced by the concrete must be matched by an identical deformation of the reinforcing bars, i.e. perfect bond is assumed; a single strain tensor is considered, representing the average strains of the composite RC material. And secondly, angle of inclination of the principal stresses coincides with the angle of inclination of the principal strains (María, 2012).

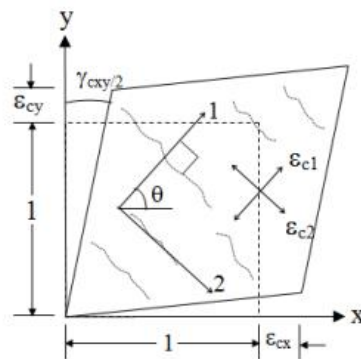
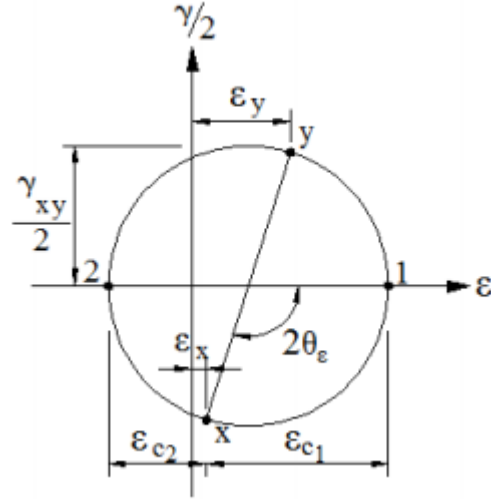


Figure 3.1 Average Concrete Strains (Güner, 2008)

The strains in the reference coordinate directions  $x$ (longitudinal) and  $y$ (transverse) can be obtained from the principal strains  $\varepsilon_1$ (= principal positive strain) and  $\varepsilon_2$ (= principal negative strain):



**Figure 3.2 Mohr's Circle of average strain (Güner, 2008)**

$$\varepsilon_x = \varepsilon_2 \cos^2 \theta + \varepsilon_1 \sin^2 \theta \quad (3.1)$$

$$\varepsilon_y = \varepsilon_1 \cos^2 \theta + \varepsilon_2 \sin^2 \theta \quad (3.2)$$

$$\gamma = 2(-\varepsilon_2 + \varepsilon_1) \cos \theta \sin \theta \quad (3.3)$$

From the above equations, the “crack” angle  $\theta$  can be derived (the cracks are assumed to be parallel to the direction of the negative principal strain):

$$\tan^2 \theta = \frac{\varepsilon_x - \varepsilon_2}{\varepsilon_y - \varepsilon_2} \quad (3.4)$$

where,  $\varepsilon_x$  is the average longitudinal strain,  $\varepsilon_y$  is the average transverse strain (positive for tension),  $\varepsilon_1$  and  $\varepsilon_2$  are the principal tensile and compressive strains, respectively, and  $\gamma$  is the average shear angle (the shear strain is half of that) on an element oriented along the x-y directions. The strain  $\varepsilon_2$  is aligned with the direction of the compressive struts, at the angle  $\theta$  to the longitudinal axis.

### 3.2 Equilibrium Conditions

Forces applied to the reinforced concrete element are resisted by both concrete stresses  $f_{cx}$  and  $f_{cy}$  and reinforcement stresses  $f_{sx}$  and  $f_{sy}$  while the applied shear stress  $\tau_{cxy}$  has to be balanced by average concrete shear stress  $v_{cxy}$ .

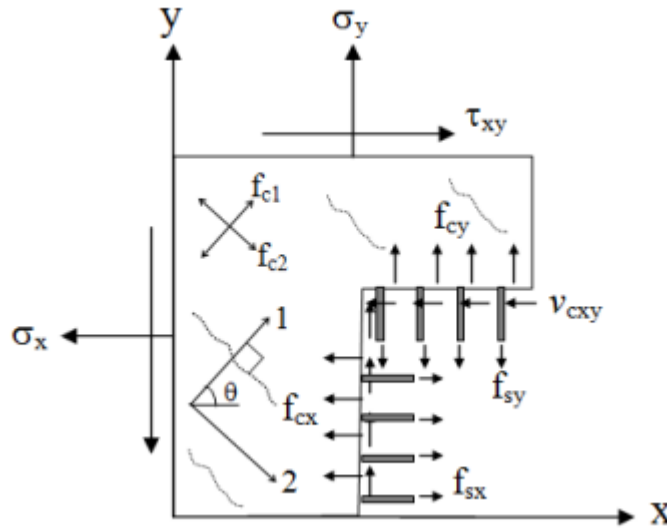


**Figure 3.3 Free Body Diagram of a Reinforced Concrete Element Showing Average stresses**  
(Güner, 2008)

$$\int_A f_x dA = \int_{A_c} f_{cx} dA_c + \int_{A_s} f_{sx} dA_s \quad (3.5)$$

Where,  $f_x$  is the external stress in the horizontal direction acting on an area  $A$ ,  $f_{cx}$  is the internal concrete stress in the  $x$  direction acting on the concrete area  $A_c$ ,  $f_{sx}$  is the stress in the reinforcement area  $A_s$  along the  $x$  direction. The areas  $A$  and  $A_c$  are slightly different because of the presence of  $A_s$ . If this small difference is ignored, equilibrium equations in the horizontal and vertical (or  $x$  and  $y$ ) directions are:

$$f_x = f_{cx} + \rho_{sx} f_{sx} \quad (3.6)$$

$$f_y = f_{cy} + \rho_{sy} f_{sy} \quad (3.7)$$

$$v_{xy} = v_c + \rho_{sy} v_{sy} = v_c + \rho_{sy} v_{sy} \quad (3.8)$$

Where  $f_y$  and  $v_{xy}$  are the normal and shear stresses in the vertical direction respectively,  $f_{cv}$  and  $v_c$  are the internal concrete stress in the y direction and the internal shear stress of the concrete, respectively, and  $f_{sy}$  is the stress in the v reinforcement. The variables  $\rho_{sx}$  and  $\rho_{sy}$  represent the geometric reinforcement ratios in the x and v direction, respectively;  $v_{sx}$  and  $v_{sy}$  are the shear stress on x reinforcement and vertical reinforcement, respectively.

From Mohr's circle applied to the average concrete stresses the following relations can be obtained:

$$f_{cx} = f_1 - \frac{v_c}{\tan \theta} \quad (3.9)$$

$$f_{cy} = f_1 - v_c \tan \theta \quad (3.10)$$

$$f_2 = f_{c1} - v_c \left( \tan \theta + \frac{1}{\tan \theta} \right) \quad (3.11)$$

Where,  $f_1$  and  $f_2$  are the average principal tensile and compressive stresses of the concrete.

### 3.3 Constitutive Relations of Concrete

The constitutive relationships relate the average strains to the average stresses, independently for each material (concrete and steel).

In MCFT (Vecchio and Collins (1986)), the stress-strain curve of a mild steel reinforcing bar is considered to be elastic-perfectly plastic with the yield stress equal to  $f_y$ .

$$f_{sx} = E_s \varepsilon_x \leq f_{yx} \quad (3.12)$$

$$f_{sy} = E_s \varepsilon_y \leq f_{yy} \quad (3.13)$$

Where,  $f_{yx}$  and  $f_{yy}$  are the strengths at yielding of the horizontal and vertical reinforcement, respectively.

However, when a reinforcing bar is surrounded by concrete, the average stress strain relationship is quite different. As a matter of fact, the bar may be at yielding in the cracked section, while in the other sections – where the concrete is still undamaged – the bar stress is lower than  $f_y$ , because a share of the tensile force resisted by the section is developed by the concrete in tension. Thus, the average stress-strain response of the reinforcement exhibits yielding at an average stress below  $f_y$ . To put it in other words, the stiffness of the embedded bar is enhanced by the concrete.

$$f_s = E_s \varepsilon_s, \text{ if } \varepsilon_s \leq \varepsilon_n \quad (3.14)$$

$$f_y(0.91 - 2B) + (0.02 + 0.25B)E_s \varepsilon_s, \text{ if } \varepsilon_s > \varepsilon_n \quad (3.15)$$

With:

$$B = \frac{1}{\rho} \left( \frac{f_{cr}}{f_y} \right)^{1.5}$$

$$\varepsilon_n = (0.93 - 2B)f_y$$

$$f_{cr} = 0.3\sqrt{f_c} \text{ (MPa)}$$

Generally, different stress-strain curves can be chosen for different types of concrete and reinforcement. Originally, Hognestad model with compression softening was suggested for normal reinforced concrete in compression proposed by Vecchio and Collins 1986. While in tension, concrete deformed elastically up to the first cracking strength, after that stress of concrete dropped following concrete tension stiffness behavior also proposed by, whereas elastic-perfect plastic response was assumed for reinforcing bars. After that many other stress-strain curves for both concrete in compression and in tension have been proposed by different researchers for different types of concrete used, and correct selection of the model (especially for concrete in tension) is necessary to obtain reliable RC response.

The MCFT is a general model for the load-deformation behavior of two-dimensional cracked reinforced concrete subjected to shear. It models concrete considering concrete



stresses in principal directions summed with reinforcing stresses assumed to be only axial. The concrete stress-strain behavior in compression and tension was derived originally from Vecchio's tests and has since been confirmed with about 250 experiments performed on two large special purpose testing machines at the University of Toronto. Similar machines have been built in Japan and the United States, providing additional confirmation of the quality of the method's predictions (Bentz, 2000).

The most important assumption in the model is that the cracked concrete in reinforced concrete can be treated as a new material with empirically defined stress-strain behaviour. This behaviour can differ from the traditional stress-strain curve of a cylinder, for example. The strains used for these stress-strain relationships are average strains, that is, they lump together the combined effects of local strains at cracks, strains between cracks, bond-slip, and crack slip. The calculated stresses are also average stresses in that they implicitly include stresses between cracks, stresses at cracks, interface shear on cracks, and dowel action. For the use of these average stresses and strains to be a reasonable assumption, the distances used in determining the average behaviour must include a few cracks. Sectional models satisfy this by needing to be at least a couple of section depths long.

A penalty for using average stress-strain relationships is that an explicit check must be made to ensure that the average stresses are compatible with the actual cracked condition of the concrete. This so-called crack check is a critical part of the MCFT and the theories derived from it. The crack check involves limiting the average principal tensile stress in the concrete to a maximum allowable value determined by considering the steel stress at a crack and the ability of the crack surface to resist shear stresses (Bentz, 2000).

As the overall stress response is based solely on average relationships, tempered with the crack-check, the method does not require an explicit calculation of dowel action force, shear stresses on crack, reinforcing stress at a crack, crack slip strains, and bond stresses. If required, the inferred values of some of these parameters may be calculated from equilibrium. The simplicity afforded by ignoring these more complex phenomena in cracked concrete is one of the strengths of the method.

### **3.4 Important Aspects of the MCFT**

#### **3.4.1 Reinforcement average response**

The MCFT assumes that the average behavior of steel can be approximated by the bare-bar response. While this is an excellent assumption prior to yield at a crack, it is not obvious that it is appropriate after first yield of the reinforcement at a crack. Note that steel first yields at a crack due to any tensile stress in the uncracked concrete needing to be balanced by extra steel stress at a crack (Bentz, 2000).

#### **3.4.2 Concrete tensile stress response ( $f_1$ )**

Concrete is assumed to be able to carry the full cracking strength prior to cracking. After cracking, tensile stresses in the uncracked concrete between the cracks will continue to stiffen the concrete, and in some cases will increase the strength. To model the high scatter behaviour of post-cracking, pre reinforcement yielding tension stiffening, a simple equation for  $f_1$  (Bentz, 2000).

#### **3.4.3 Concrete compressive stress response ( $f_2$ )**

Uncracked concrete in compression is assumed to follow the cylinder stress-strain curve. The stress-main curve is a parabola, a function of the principal compressive strain ( $\epsilon_2$ ), as well as the principal tensile strain ( $\epsilon_1$ ). The tensile strain component models the decrease in apparent concrete compressive strength observed in tests when the concrete was transversely cracked. This often controls the strength of beams with stirrups (Bentz, 2000).

#### **3.4.4 Crack width ( $\omega$ )**

When subjected to shear, new cracks may form old cracks may close or become inactive. This complex load-history dominated behaviour is simplified to only a single set of parallel cracks forming at the average angle of principal compressive stress. The spacing of the cracks ( $s_\theta$ ) is calculated with the shown equation that converts the calculated crack spacing in the two orthogonal directions to an estimated diagonal spacing. It is recommended that these crack spacings in the base X and Y directions be estimated, based on the method in Collins and Mitchell. Crack widths are assumed to be simply the product of the principal tensile strain and the crack spacing (that is, elastic strains in the uncracked concrete between the cracks are ignored) (Bentz, 2000).

### 3.4.5 Shear on the crack ( $v_{ci}$ )

It is assumed that there is a limiting interface shear stress on a crack that can be transmitted before the crack begins to slip. This shear on the crack limit is higher for stronger concrete or larger aggregates (variable  $a$ ). Increasing crack widths lower the maximum allowed shear on the crack (Bentz, 2000).

Note that shear on the crack interface,  $V_d$ , is not an average stress, but a local one. Recall that the MCFT calculates the total element force state with average stresses at angle  $\theta$ . The calculated shear on the crack is resisted by a crack also assumed to be at an angle of  $\theta$ . This indicates that there must be a local deviation in angle of principal stress at a crack if there is to be any shear on the crack (Bentz, 2000).

### 3.4.6 Local reinforcement stress at a crack ( $f_{scrx}$ , $f_{scry}$ )

Calculation of this term defines the crack check. Note that there are two equations, one for each direction of reinforcement, derived as a sum of forces in the X and Y directions locally at a crack. Clearly, the steel stress at a crack must be lower than some limit, usually the yield stress (Bentz, 2000).

### 3.4.7 The Crack Check

The crack-check in the Modified Compression Field Theory (MCFT) represents an explicit check to ensure that the average stress levels can be resisted locally at a crack. It has become apparent, in the past, that some researchers and engineers have implemented the MCFT without including the crack-check. This is unconservative and potentially unsafe. In a series of papers, for example, Hsu has shown that ignoring the crack-check can produce results that are very unconservative indeed.

The need for the crack check is easy to demonstrate. Consider the free body diagram shown in Figure 3.4 with the left half of the element drawn with average stresses as used in the MCFT and the right half with local stresses at crack where there will be no concrete tension (Bentz, 2000).

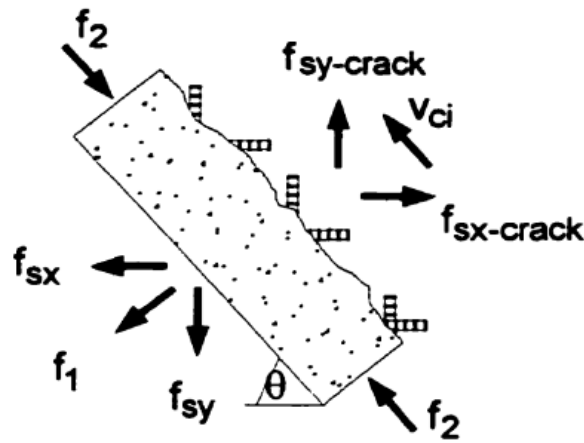


Figure 3.4 Two dimensional crack check (Bentz, 2000)

Note that, in MCFT the crack check must be performed to ensure that the stress in the reinforcement does not exceed the strength limit at the crack interface. On the contrary, if the embedded-reinforcement stress-strain model is used, no checks on cracking are necessary, because all the constitutive relations are based on average values in the steel, and therefore  $f_y$  cannot be exceeded in any section (María, 2012).

Recalling that the MCFT, for simplicity, uses the same stress-strain curve for steel at a crack and on average, it is possible, indeed common, for both  $f_{srx}$  and  $f_{sry}$  & crack to equal  $f_y$ , the bare-bar yield stress. From the free body diagram, it is clear that the concrete tensile stress,  $f_1$ , must equal zero in this case. Ensuring that the local stresses at a crack not exceed the yield stress in this case is the job of the crack check. For reinforcement with, for example, a biaxial stress-strain response, it can be assumed that the stress at a crack will always be able to achieve at least the stress corresponding to the bare-bar stress at the given average strain (Bentz, 2000).

$$\underbrace{A_s \cdot f_y}_{\text{crack\_location}} = \underbrace{A_s \cdot f_{s,av} + A_{c,ef} \cdot f_{ct,av}}_{\text{average\_section}} \quad (3.16)$$

### 3.5 Sectional-Based Analysis of Concrete Structures

Engineering analysis can take many forms in a spectrum of complexity. At one end are hand and graphical methods of analysis that tend to be laborious, yet are good for developing an

understanding of the solution technique to the problem at hand. At the other end of the spectrum are general-purpose, non-linear, finite element computer programs. These are far more powerful, yet they are sufficiently complex that it is generally necessary to take it on trust that they work properly. One generally does not do calculations to determine if moment equilibrium is maintained in a frame or if the calculated loads really can be carried by the cross section, for example. The input and output from these complex programs tend to be difficult to understand and verify.

In between these two extremes of analysis lies sectional analysis. This is a familiar topic to engineers as the idea is strongly embedded in codes of practice. The units of currency for a sectional analysis are the familiar concepts of axial load, moment and shear. This means that they do the analysis at one location in a beam or plate and calculate the strength and deformation in terms of moments, shear, curvatures, etc. Generally, the only assumption needed to make a sectional analysis is something akin to the familiar assumption "plane sections remain plane" of engineering beam theory (Bentz, 2000).

In using the sectional analysis approach, the problem of determining the response of a reinforced concrete structure to applied loads is broken up into two interrelated tasks.

First, the sectional forces at various locations in the structure caused by the applied loads are determined. This step is usually performed assuming that the structure remains linearly elastic. Then the response of a local section to the sectional forces is determined. In this second step, which is the sectional analysis, the non-linear characteristics of cracked reinforced concrete are taken into account.

$$\varepsilon_{c1} = \frac{L - L_o}{L} \quad (3.17)$$

$$\phi = \frac{\phi_i - \phi_{i+1}}{L} \quad (3.18)$$

$$\varepsilon_{x,top} = \varepsilon_{c1} - \frac{h_s}{2} \phi \quad (3.19)$$

$$\varepsilon_{x,bot} = \varepsilon_{c1} + \frac{h_s}{2} \phi \quad (3.20)$$

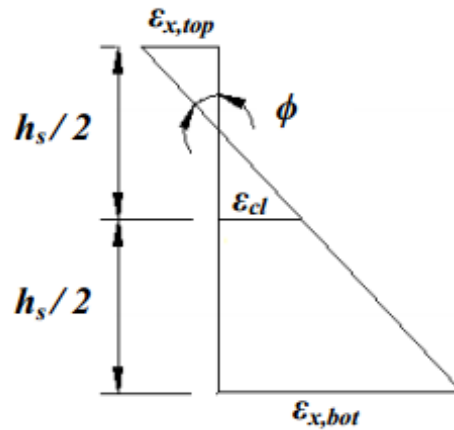


**Figure 3.5 Longitudinal Strain Distribution**

The response of each reinforced or prestressed concrete section to mechanical loads is determined using a layered section approach in which the cross section is divided into a number of concrete layers, longitudinal reinforcing bar layers and longitudinal prestressing steel layers (Figure 3.6). The procedure requires supply of the concrete layer widths,  $b_i$  and heights,  $h_i$ , reinforcing and prestressing steel areas,  $A_{sj}$ , and basic mechanical properties of concrete, reinforcing steel (longitudinal and transverse) and prestressing steel (longitudinal) as shown in Figure 12 (Güner, Serhan, 2008).

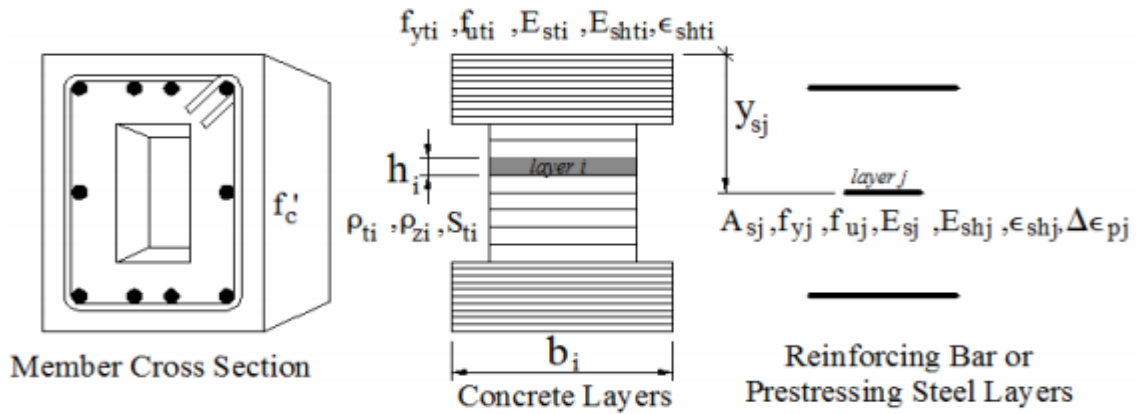


**Figure 3.6 Input Parameters for Sectional Analysis (Güner, 2008)**

In Figure 3.6,  $f'_c$  is the concrete compressive strength,  $\rho_{ti}$  and  $\rho_{zi}$  are the transverse and out-of-plane reinforcement ratios respectively,  $S_{ti}$  is the spacing of the transverse reinforcement in the longitudinal direction,  $f_{yi}$  and  $f_{titi}$  are the yield and ultimate stresses of the transverse reinforcement respectively,  $E_{sti}$  and  $E_{shti}$  are the Young's and the strain hardening moduli of the transverse reinforcement,  $\epsilon_{shti}$  is the strain at the onset of strain hardening,  $A_{sj}$  is the total cross-sectional area of the longitudinal reinforcement, and  $\Delta\epsilon_{pj}$  is the locked-in strain for a prestressing steel layer (Güner, Serhan, 2008).

Each concrete layer and steel element is then analyzed individually based on the MCFT or the DSFM, although sectional compatibility and sectional equilibrium conditions are satisfied as a whole. The main sectional compatibility requirement enforced is that plane sections must remain plane, while the sectional equilibrium requirements include balancing the axial force, shear force and bending moment which are calculated by the global frame analysis. An assumption regarding the shear strain or shear flow distribution is also made as explained below. In addition, the clamping stresses in the transverse direction are assumed to be zero, which permits the calculation of the total concrete strains in the transverse direction in a shear-strain-based analysis, or the axial concrete stresses in a shear-strain-based analysis.

In this layered representation of a cross section, the 'plane sections remain plane' hypothesis permits the calculation of the longitudinal strain in each layer of concrete, reinforcing steel and prestressing steel as a function of the top and bottom fibre strains (Figure 3.5). It is further assumed that the strains in each layer are uniform and equal to the strains at the centre of the layer (Figure 3.7). Therefore, the longitudinal strain distribution (Figure 3.5) can

simply be determined from the axial deformation and curvature values calculated by the global frame analysis (Güner, Serhan, 2008).

There are basically two different procedures available, a shear-stress-based analysis, and a shear-strain-based analysis. In the shear-strain-based analysis, the average shear strain for each member is calculated and is distributed across the cross section depth. In this approach, the strain in the transverse direction,  $\epsilon_y$ , must converge to find the required axial stresses in the concrete layers,  $\sigma_{cx}$ , at the end of the sectional calculations. Shear-stress-based analysis, a uniform shear flow is assumed across the cross section depth and the corresponding shear strains of the layers are calculated through sectional calculations (Güner, Serhan, 2008).

Based on these two procedures, five different shear analysis options are available. They are: (0) Shear not Considered, (1) Uniform Shear Flow Distribution (Multi-Layer Analysis), (2) Uniform Shear Strain Distribution (Multi-Layer Analysis), (3) Parabolic Shear Strain Distribution (Multi-Layer Analysis), and (4) Parabolic Shear Strain Distribution (Single-Layer Analysis) (Figure 3.7) (Güner, Serhan, 2008).

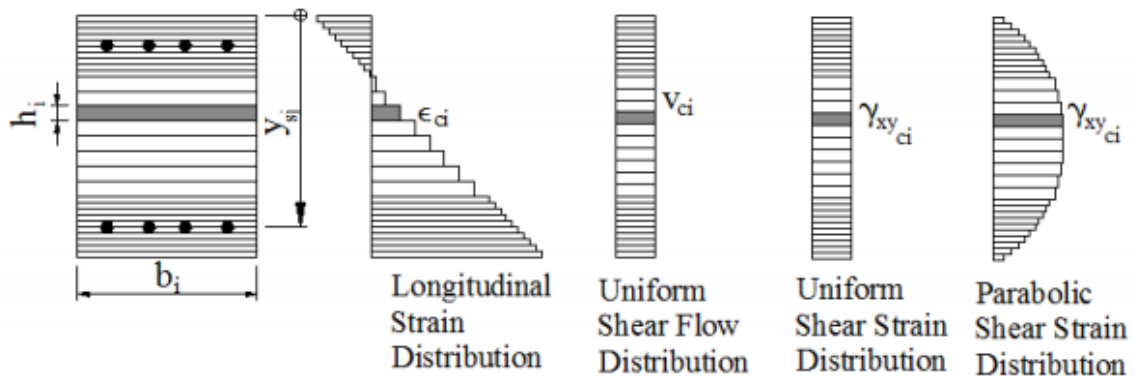


**Figure 3.7 Longitudinal and Shear Strain Distribution across Cross Section Depth**

### 3.5.1 Types of Sectional Analyses

There are about 6 different types of sectional analyses. These include uniaxial stress-strain analysis, biaxial stress strain relation analysis and triaxial stress strain analysis. These differ on the level of numerical integration of the analysis. Accordingly these calculate behavior at a point, along a line and over an area respectively.

The modeling assumptions in the implementation of sectional analysis including shear are first that engineering beam theory is valid. That is, a straight line drawn on the element



before deformation will still be a straight line after deformation. The second assumption is that there is no significant net stress in the transverse direction. This means that the concrete and transverse steel forces must balance at each point through the depth of the element. Both these assumptions are good ones when the analysis is being performed a distance away from the support and the load point. Close to the load and to the reactions, however, there will be a transverse clamping stress from the application of the load itself which will tend to locally increase the strength. This is one reason that short beams are noticeably stronger in shear than long beams with the same cross section.

### **3.5.2 Secant Stiffness Formulation**

With MCFT sectional analysis, a beam section is discretized into  $m$  fibers and  $n$  longitudinal reinforcing bars. Each concrete fiber is treated separately as a new orthotropic material having its own stress-strain characteristics and satisfaction of three conditions are required including equilibrium, compatibility, and constitutive relations. In the originally developed method implemented in program SMALL by Vecchio, finding stress/strain values of each fiber involved two-loop iteration process of square root and trigonometric equations occasionally causing instability and is time-consuming (Chan, 2008).

In the consideration of shear effect in the section, Vecchio proposed three different approaches: rigorous dual section, approximate constant shear flow distribution, and approximate parabolic shear strain distribution.

Dual section provides exact solution with varying shear strain and shear flow distribution across the section; however, the approach involves the analysis of second section at a small distance ( $h/3$ ) from the first section to find shear flow equilibrium. Assumed constant shear flow and parabolic shear strain distribution; on the other hand, were reported as shown in Figure 3.8 to provide very close results and much quicker computation time. As the consequence, parabolic shear strain distribution is assumed herein.

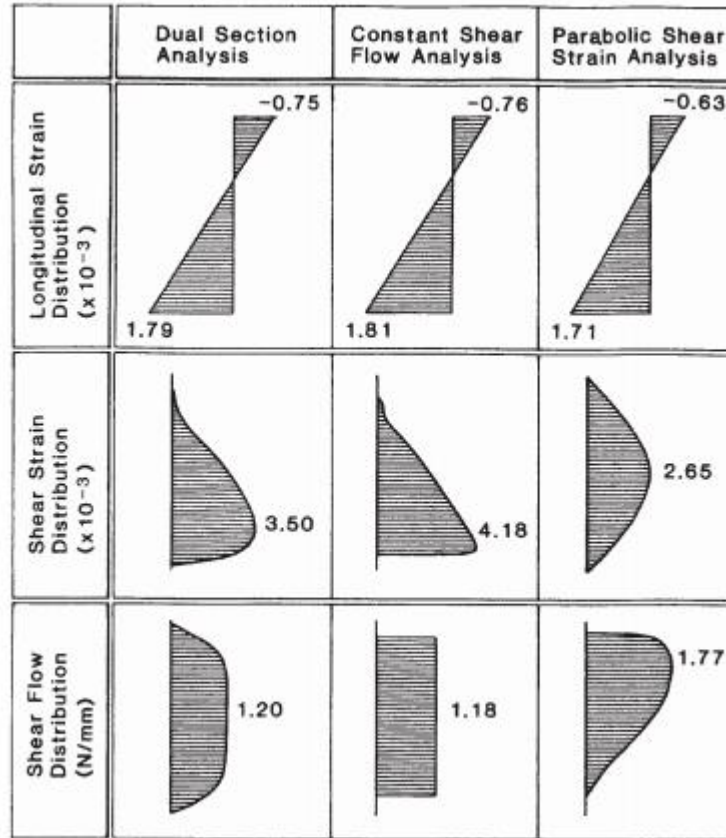


Figure 3.8 Shear flow and shear strain based on Vecchio's rigorous and approximate approaches (CHAN, 2008)

After longitudinal stresses  $\sigma_x$  and shear stresses  $\tau_{xy}$  are found, section forces  $N$ ;  $M$ ;  $V$  can be determined from sectional equilibrium of concrete and longitudinal reinforcement as follows:

$$N = \sum_{i=1}^m \sigma_{xi} b_i h_i + \sum_{j=1}^n f_{sxj} A_{sxj} \quad (3.21)$$

$$M = \sum_{i=1}^m \sigma_{xi} b_i h_i (y_{ci} - \bar{Y}) + \sum_{j=1}^n f_{sxj} A_{sxj} (y_{sj} - \bar{Y}) \quad (3.22)$$

$$V = \sum_{i=1}^m v_{xyi} b_i h_i \quad (3.23)$$

### 3.5.3 The Longitudinal Stiffness Method

While most sectional analysis programs do not include the effects of shear stresses that vary through the depth of the element, it is necessary to include the effects of beam shear stress and the effects of out-of-plane shear stresses, which both vary through the depth of the element. The challenge is to determine the distribution of shear stress with depth. It will be affected by the width of the section, the material properties of the concrete, and the location and amount of reinforcement. The technique used is based on equilibrium of longitudinal stresses as derived by Jourawski in 1856 (Bentz, 2000).

This method is an extension of the methods used by earlier nonlinear sectional analysis programs extended to increase performance and computational stability.

#### 3.5.3.1 Traditional Shear Stress Calculation

Consider the prismatic beam on simple supports shown in Figure 3.9. The right side of the figure is a free body diagram of the part of the beam between sections A and B.

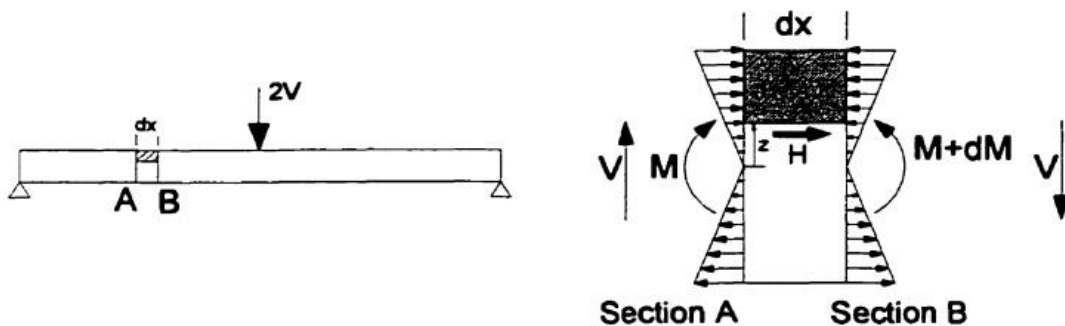
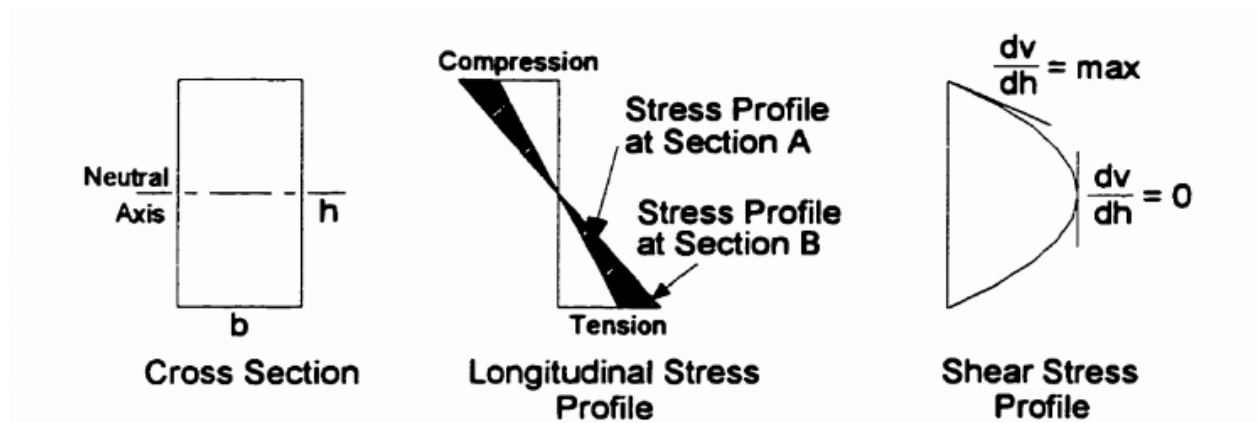


Figure 3.9 Shear stress calculation (Bentz, 2000)

Consider the shaded portion at the top right of Fig 3.9 as a free body diagram of the top of the beam, from elevation  $z$  up to the top of the beam. It is subjected to a force on the left from the moment, but a higher force on the right from the slightly higher moment. This requires a balancing force on the cut plane of the beam, shown as  $H$ . Due to the summation of moments about a point equaling zero, the shear stress in a horizontal plane at a point must equal the vertical shear stress. As such, the force  $H$  divided by the beam width and  $dx$  results in the vertical shear stress on the beam at depth  $z$ .

$$v = \frac{V.Q}{I.b} \quad (3.24)$$

An implicit assumption in this theory is that plane sections remain plane it was used to calculate the longitudinal stresses. Though the shear strains associated with the calculated shear stress will warp the section, violating plane sections, the warping does not affect the longitudinal stress gradient for regions of constant shear.



**Figure 3.10 Internals of shear stress calculation**

In this case, the difference in longitudinal stresses between sections A and B is linear, so the shear stress profile is parabolic. For general nonlinear materials, however, the difference in longitudinal stress profiles will not necessarily be linear. The difference in strains between sections A and B, on the other hand, will always be linearly distributed over the depth when the assumption of plane sections remaining plane is used. If this change in longitudinal strain profile is known along with the longitudinal stiffness (i.e. rate of change of longitudinal stress with longitudinal strain) over the height of the beam, the shear stress profile can be generated (Bentz, 2000).

### 3.6 Solving problems with the MCFT

Two classes of questions arise with general shear models such as the MCFT. The first is to find a stress state corresponding to a strain state, and the second is to calculate a strain state corresponding to a stress state. The second is much more difficult as it must be solved via numerical iteration (Bentz, 2000).

## Solution of MCFT Equations

Determining stresses given strains using MCFT equations is an easy task; however, calculating strains from given forces is tedious and requires trial-and-error. For the latter case, two unknowns are estimated in the beginning and solving equations verifies whether the estimated values are correct or need to be changed. For example, one solution strategy is to estimate concrete stresses in the x and z-directions. Then, calculate steel stresses in the x and z-directions in addition to concrete angle of inclination  $\theta$  and principal stresses from equilibrium equations. Subsequently, determine strains in the principal, x and z-directions using material constitutive laws for concrete and steel. At this stage, crack equilibrium conditions should be checked and principal tension strain should be adjusted accordingly. The calculated strains should then satisfy compatibility equations otherwise the estimated concrete stresses should be revised and the procedure should be repeated until compatibility equations are satisfied (Esfandiari, 2009).

Two procedures were developed using the modified compression field theory, MCFT, to predict the shear capacity of the test beams. These procedures are outlined in this section. The first procedure, called the response procedure, gives the full force stress-strain response of the member subjected to moment and shear. The procedure uses an iterative process to reach a solution. The design procedure is also iterative, but is simpler than the response procedure (Gregory P. Pasley, December 1990).

### 3.6.1 Response Procedure using MCFT

The MCFT (Vecchio and Collins 1986) can be implemented in different ways with varying levels of complexity, from a full, nonlinear finite-element analysis, to a multilayer sectional analysis that accounts for the variation of crack width over the section (Vecchio and Collins 1988), to the simplest case where only the crack width at the level of the flexural tension reinforcement is considered (Collins and Mitchell 1991). The latter case, which is most suitable for design, is analogous to a variable-angle truss model with diagonal concrete tension ties.

The relationships from the modified compression field theory, are used to obtain the shear response of a member. The shear response is expressed in terms of principal tensile strain,  $\epsilon_1$ ,

and the shear force corresponding to  $\varepsilon_1$ . Values of  $\varepsilon_1$  are gradually increased to obtain the behavior (Gregory P. Pasley, December 1990).

The procedure is

Step 1 - Choose a value of  $\varepsilon_1$ , at which to perform the calculations.

Step 2- Estimate principal compressive stress direction  $\theta$ .

Step 3- Calculate average crack width  $\omega$

$$\omega = \varepsilon_1 S_\theta \quad (3.25)$$

$$S_\theta = \frac{1}{\frac{\sin \theta}{s_{mx}} + \frac{\cos \theta}{s_{my}}} \quad (3.26)$$

in which  $s_{mx}$  and  $s_{my}$  are crack spacings along the longitudinal and shear reinforcement and are defined as:

$$s_{mx} = 2(c_x + \frac{s_x}{10}) + 0.25k_1 \frac{d_{bx}}{\rho_x} \quad (3.27a)$$

$$s_{my} = 2(c_v + \frac{s_x}{10}) + 0.25k_1 \frac{d_{by}}{\rho_y} \quad (3.27b)$$

in which,

$s_{mx}$  is crack control parameter of x-direction reinforcement,

$s_{my}$  is crack control parameter of y-direction reinforcement

$c_x$  is the vertical distance from the neutral axis of the **uncracked** section to the inside edge of the tension steel,

$C_v$  is the horizontal distance from the center of the web to the Inside edge of the stirrup,

$d_{bx}$  is the diameter of the longitudinal steel,

$d_{by}$  is the diameter of the stirrups,

$s_x$  is the horizontal clear space between the longitudinal bars,

$s$  is the stirrup spacing,

$$\rho_x = A_s / A_c$$

$k_1$  is 0.4 for deformed bars and 0.8 for smooth bars.

For members with at least minimum amount of reinforcement, crack spacing may be conservatively assumed as  $s_0=300$  mm (Esfandiari, 2009).

Step 4-Estimate average stress in weaker reinforcement; assume that this is the y-reinforcement. Hence, estimate  $f_{sy}$ .

Step 5-Calculate average tension in the concrete  $f_{c1}$ ,

$$f_{c1} = E_c \cdot \varepsilon_t, \quad \text{if } \varepsilon_t \leq \varepsilon_{cr} \quad (3.28a)$$

$$f_{c1} = \frac{f_{cr}}{1 + \sqrt{200\varepsilon_1}}, \quad \text{if } \varepsilon_t > \varepsilon_{cr} \quad (3.28b)$$

$$E = \frac{2f'_c}{e'_c}$$

$$f_{c1} \leq v_{ci \max} (0.18 + .3k^2) \tan \theta + \rho_{xy} (f_{yy} - f_{xx}) \quad (3.28c)$$

$$k = (1.64 - \frac{1}{\tan \theta}) \geq 0$$

$$v_{ci \max} = \frac{\sqrt{-f_{ci}}}{0.31 + \frac{24\omega}{a+16}} \quad (3.28d)$$

Step 6 - Calculate the shear load on the section,  $V$

$$V = f_{c1} b_w j d \cot \theta + A_v f_v \cot \theta / s \quad (3.29a)$$

$$jd = \frac{d - (M/ f_c' - V_u \cot \theta)}{1.70 f_c' b} \quad (3.29b)$$

Step 7 - Calculate the principal compressive stress,  $f_{c2}$ . If  $f_2$  exceeds  $f_{2,max}$ , the iteration is terminated because  $\varepsilon_1$  is too large.

$$f_{c2,max} = \frac{f_{c2}}{\left( 2 \left( \frac{\varepsilon_2}{\varepsilon_c'} \right) - \left( \frac{\varepsilon_2}{\varepsilon_c'} \right)^2 \right)} \quad (3.30a)$$

$$f_{c2,max} = \frac{f_c'}{0.8 - .34 \frac{\varepsilon_1}{\varepsilon_c}} \leq 1.0 \quad (3.30b)$$

$$\varepsilon_c' = -0.002$$

Step 8 - Calculate the principal compressive strain,  $\varepsilon_2$

$$\varepsilon_2 = \varepsilon_c' \left( 1 - \sqrt{1 - \frac{f_{c2}}{f_{c2,max}}} \right) \quad (3.31)$$

Step 9 - Calculate the longitudinal strain in the web,  $\varepsilon_x$ , and the strain in the web reinforcement,  $\varepsilon_y$ . Note,  $\varepsilon_x$  is calculated at the mid height for members which contain stirrups, and at the level of the tension steel in members which contain no stirrups.

$$\varepsilon_x = \frac{\varepsilon_2 + \varepsilon_1 \tan^2 \theta}{1 + \tan^2 \theta} \quad (3.32a)$$

$$\varepsilon_y = \frac{\varepsilon_1 + \varepsilon_2 \tan^2 \theta}{1 + \tan^2 \theta} \quad (3.32b)$$

Step 10 - Calculate  $f_{sy}$

$$f_{sy} = E_s \cdot \varepsilon_y \leq f_{yy} \quad (3.33)$$

Step 11- Check to see if the calculated value of  $f_{sy}$  in step 10 equals the value of  $f_{sy}$  estimated in step 4. If it does not, go back to step 4 and revise the estimate of  $f_v$ .



Step 12\*: Find axial forces due to the moment which occurs at the shear, V, calculated in step 6. This is done using moment-curvature relationships in the following procedure:

Step 12a\*: Set moment equal to the shear, V, times the ratio M/V. This ratio will be constant throughout the loading of the beam for these cases, and is dependent upon the loading and beam geometry.

Step 12b\*: Assume a linear strain distribution across the concrete section, and choose a strain at the extreme compressive fiber of the concrete,  $\epsilon_{ct}$ .

Step 12c\*: The distribution of compressive stress in the concrete can be represented by an equivalent stress block with an average stress of  $\alpha_1 f'_c$  and a depth of  $\beta_1 c$ , in which c is the distance from the extreme compressive fiber to the neutral axis of the section. The equations used for  $\beta_1$  and  $\alpha_1 \beta_1$  are:

$$\beta_1 = \frac{4 - \frac{\epsilon_{ct}}{\epsilon_2}}{6 - \frac{\epsilon_{ct}}{\epsilon_2}} \quad (3.34)$$

$$\alpha_1 \beta_1 = \frac{\epsilon_{ct}}{\epsilon_2} - \frac{1}{3} \left( \frac{\epsilon_{ct}}{\epsilon_2} \right)^2 \quad (3.35)$$

In which  $\epsilon_2$  is the strain at  $f'_c$ .

Step 12d\*: Calculate the distance from the compression face to the neutral axis, c, using the flexural lever arm, jd, calculated in step 6.

$$c = \left( d - \frac{jd}{2} \right) - x \quad (\text{for beams with stirrups})$$

$$c = d - x \quad (\text{for beams without stirrups})$$

in which x is the distance from the point where  $\epsilon_x$  is measured to the neutral axis and is given by:

$$x = \frac{\epsilon_x \left( d - \frac{jd}{2} \right)}{\epsilon_x + \epsilon_{ct}} \quad (\text{for beams with stirrups})$$

$$x = \frac{\varepsilon_x d}{\varepsilon_x + \varepsilon_{ct}} \quad (\text{for beams without stirrups})$$

Step 12e\*: Calculate the tension force, T, and compression force, C, in the concrete.

$$T = \varepsilon_x E_s A_s \leq A_s f_{yd} \quad (3.36)$$

in which  $\varepsilon_s$  is the strain in the tension steel, which is given by

$$\varepsilon_s = \varepsilon_{ct} \frac{d-c}{c} \quad (\text{for beams with stirrups})$$

$$\varepsilon_s = \varepsilon_{ct} \quad (\text{for beams without stirrups})$$

and

$$C_c = \alpha_1 \beta_1 b_w c f'_c$$

Step 121\*: Calculate the moment about the point that is  $jd/2$  from the tensile steel.

$$M = T \left( \frac{jd}{2} \right) + C_c \left( d - \frac{jd}{2} - \frac{\beta_1 c}{2} \right) \quad (3.37)$$

Step 12g\*: Check to see if the moment in step 12f equals the moment obtained in step 12a. If not, go back to step 12b and choose a new  $\varepsilon_1$ .

Step 13\*: Calculate the net axial load, N, at the cross-section using:

$$N = T + f_{c1} b_w jd - (C_c + V \cot \theta) \quad (3.38)$$

Step 14: Check to see if the section is in equilibrium,  $N=0$ . If not, return to step 2 and re estimate  $\varepsilon_1$ . If N does equal zero, then the shear calculated in step 6 corresponds to the value of  $\varepsilon_1$  chosen in step 1. To obtain the entire response for the member, return to step 1 and choose a new  $\varepsilon_1$ .

Once a complete response is obtained, the nominal shear capacity of the member is taken as the peak shear attained on the response curve.

### 3.6.2 Design Procedure Using MCFT

The design procedure is based on the response procedure. As presented by Collins and Mitchell (22), the design procedure uses several assumptions to develop a design table which can be used to predict the capacity of a member. Portions of the design tables developed by Collins and Mitchell are given in Table.

These tables were developed using the assumptions that the maximum size of aggregate,  $a$ , used to calculate  $V_{ci}$ , is 19mm ( 0.75 inches) and, for the beams with stirrups,  $S_{m\theta}$  is equal to 300mm (12 inches). For all beams,  $\varepsilon_x$  is taken at the level of the flexural reinforcement. These assumptions are made to give conservative results. The design procedure is an iterative process and proceeds as follows for a fixed value of  $M/V$ :

1: Estimate the nominal shear capacity,  $V_n$  and the crack angle,  $\theta$ .

Step 2: Calculate the height of the compressive stress block,  $a$ . The following equation is

$$a = V_u \frac{\left(\frac{M/V}{jd} - \cot \theta\right)}{0.85 f'_c b} \quad (3.39)$$

$$jd = d - a / 2 \quad (3.40)$$

Step 3: Calculate  $\varepsilon_x$  using the equation given by Collins and Mitchell

$$\varepsilon_x = V \frac{\left(\frac{M/V}{jd} - 0.5 \cot \theta\right)}{E_s A_s} \quad (3.41)$$

In which  $\varepsilon_x \leq f_{yd} / E_s$

Step 4: For beams with stirrups, calculate  $v/f'_c$ , in which  $v = V_n/(b_w jd)$

Step 5: Use the design tables to determine  $\beta$  and  $\theta$ .

Step 6: Determine the nominal shear capacity of the member using the following equations:

$$V_n = V_c + V_s \quad (3.42)$$

In which

$$V_c = \beta \sqrt{f'_c} b_w j d \quad (3.43)$$

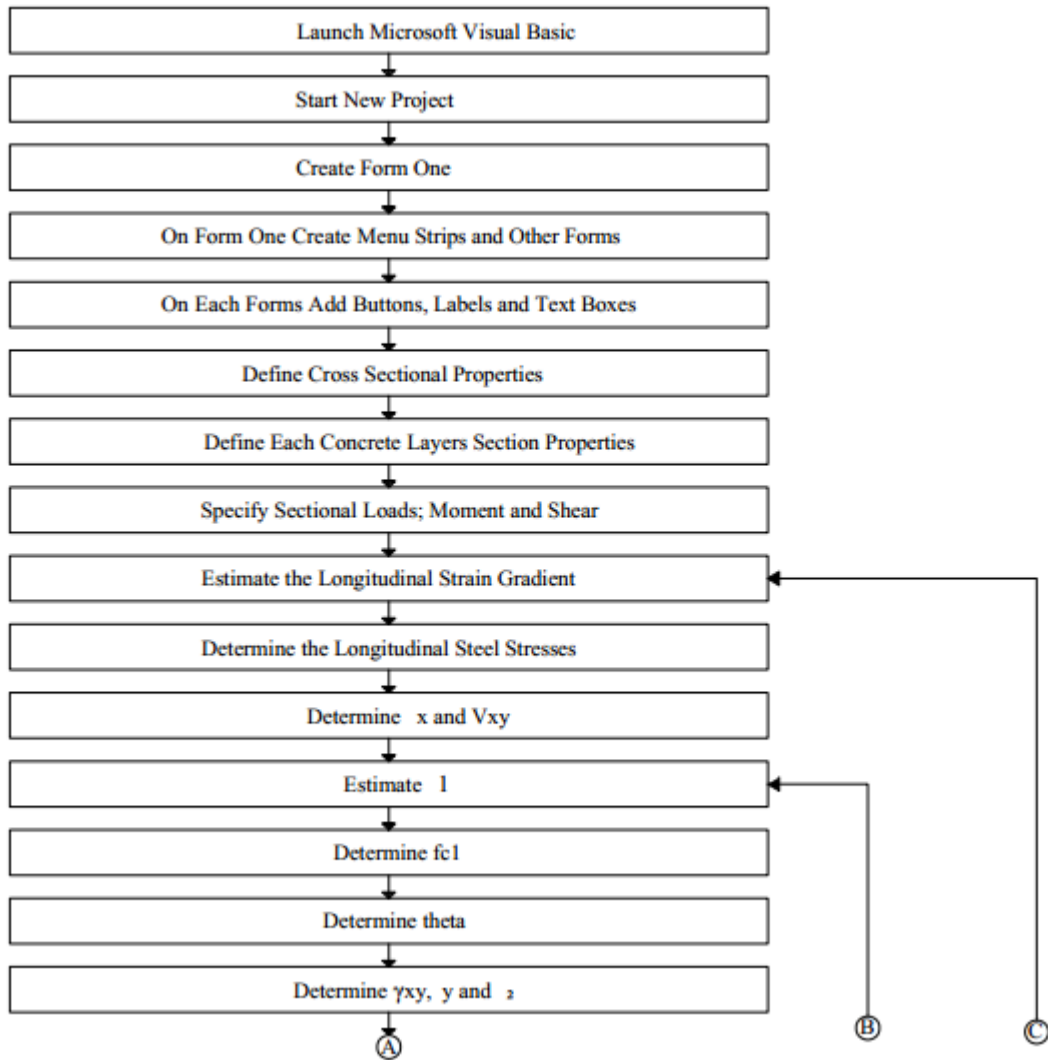
$$V_s = \rho_v f_{vy} b_w j d \cot \theta \quad (3.44)$$

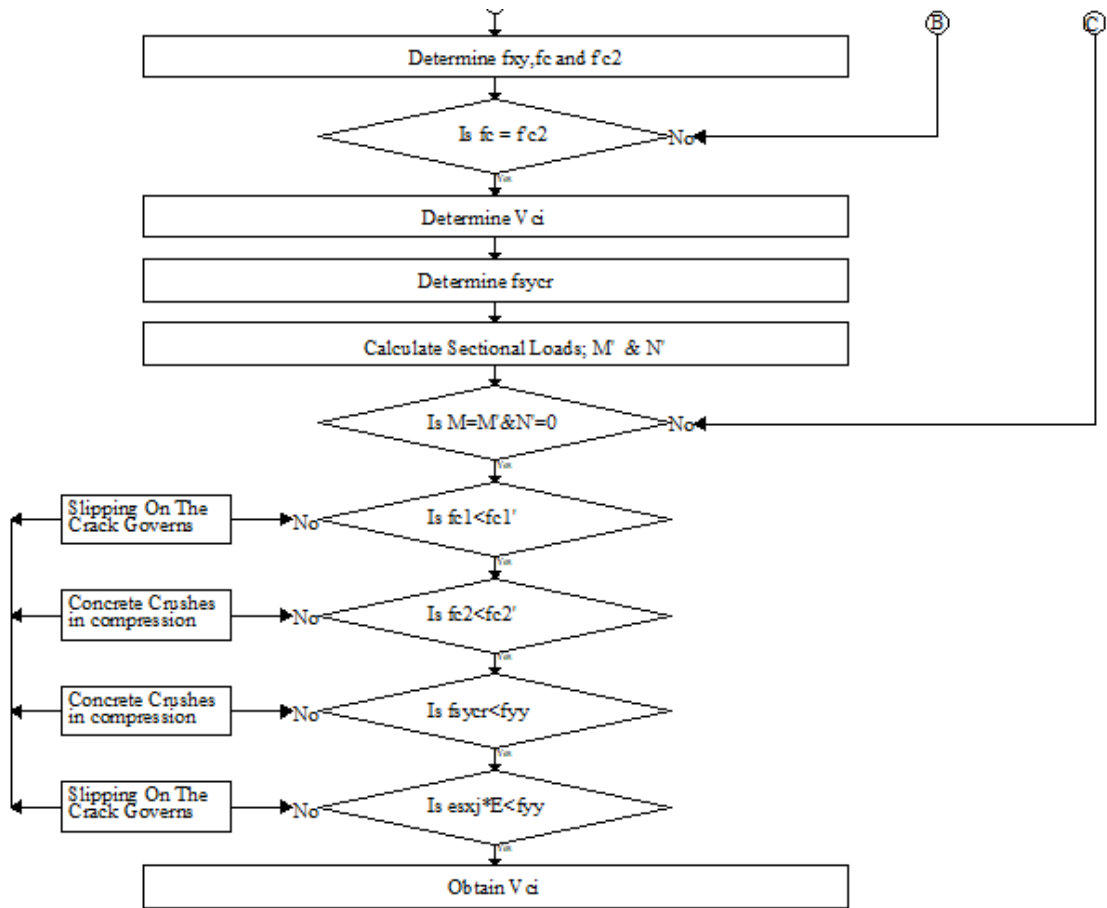
Step 7: Compare the  $V_n$  and  $\theta$  from step 7 to the  $V_n$  and  $\theta$  estimated in step 1. If they are not equal, go back to step 1 and reestimate  $V_n$  and  $\theta$ .

This procedure continues until the  $V_n$  and  $\theta$  estimated match those which are obtained from the tables. This procedure gives the nominal shear capacity of the member, not a full shear response of the member.

## Chapter 4 ANALYSIS AND ALGORITHMS DEVELOPMENT

### 4.1 Algorithms Development





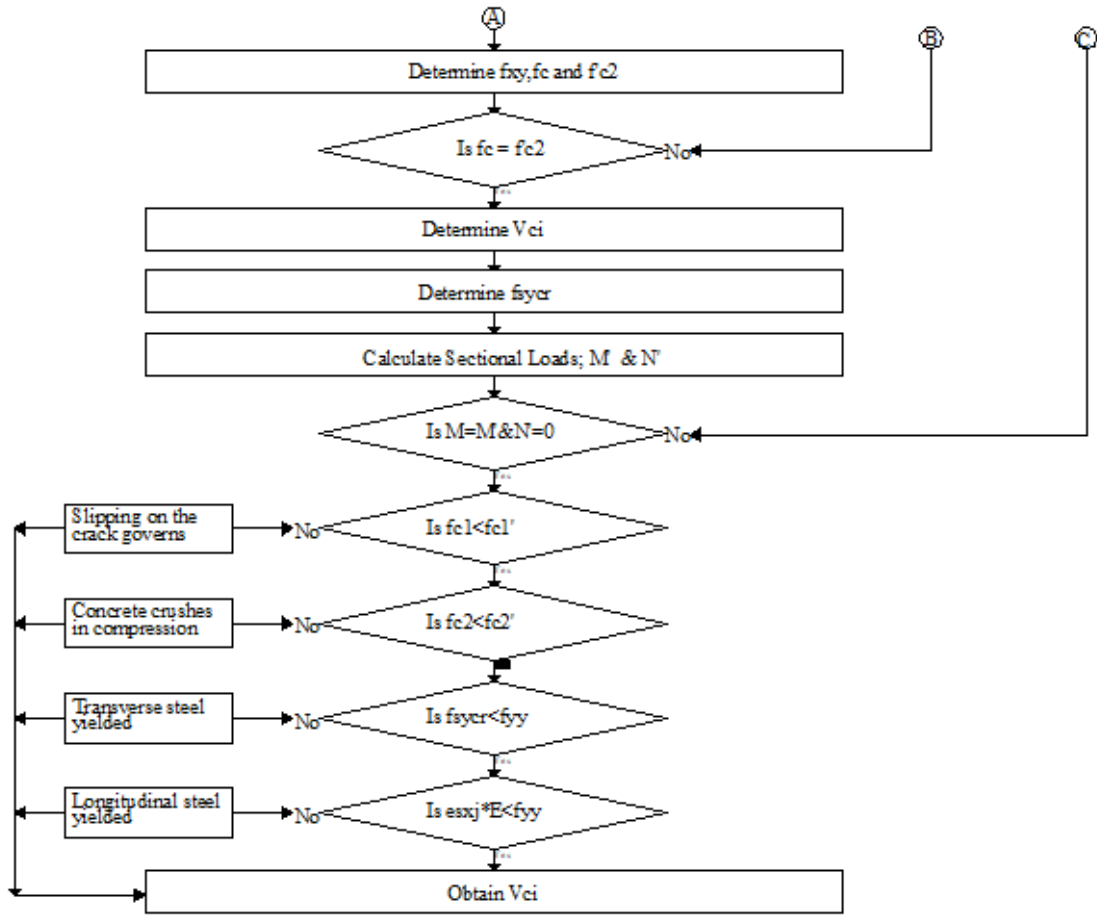


Figure 4.1 Flow chart

## 4.2 Analysis

Any beam sections can be analyzed using a windows form application developed on Microsoft Visual Basic 2015 based on MCFT method. And the results are to compared with the values of Euro and ACI codes.

Consider the following simply supported, cantilever and propped beams with different loading conditions. In order to see the differences clearly, the beams were analyzed for the same section in each of the codes and the MCFT.

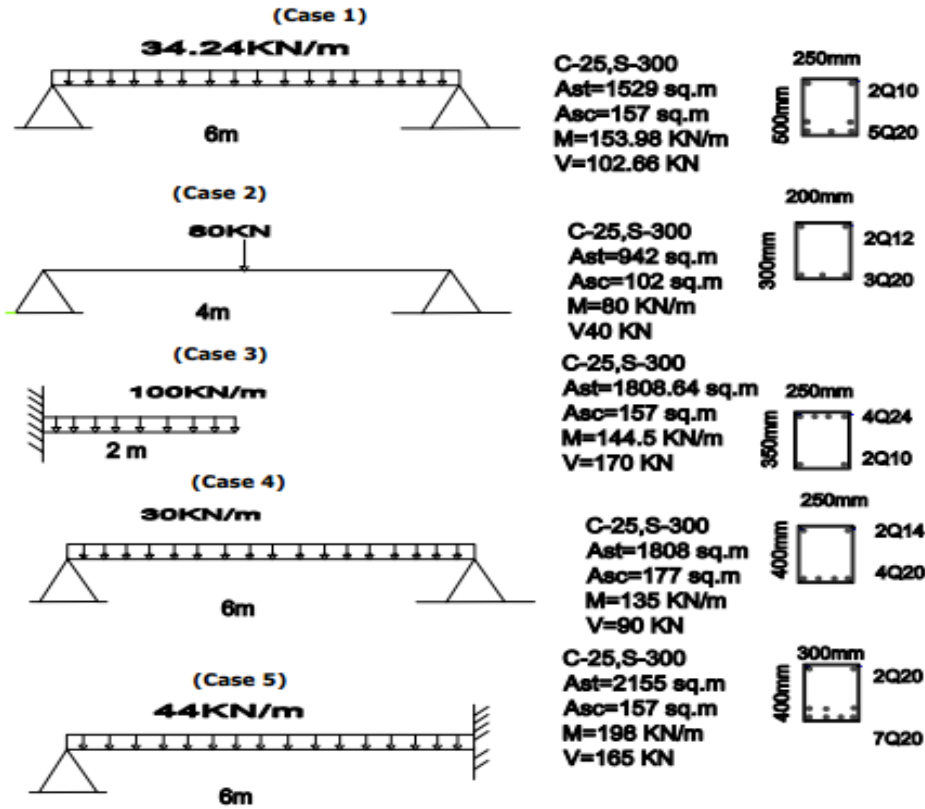


Figure 4.2 Beam sections used for shear capacity comparison

In the proceeding figures the necessary information regarding the beams is given. In the coming pages design of three of these beams for shear according to Euro code and ACI code is shown in the coming pages and the rest two are not shown to avoid detail calculation. The shear design of the rest beams was performed by excel template and is not shown this thesis.

#### 4.2.1 Shear Design Procedure Using Euro Code

##### Case 1 a simply supported beam subjected to uniform loading

The critical shear section is at  $d$  distance from the support.

Using 25mm concrete cover and  $\varnothing 8$  for shear reinforcement, the structural depth can be calculated as

$$d = D - \phi / 2 - \phi_{stirrup} - cover$$

$$d = 500 - 25 - 8 - 10 = 457 \text{ mm}$$



$$V_{ED} = 102.66 \left( \frac{3 - .2 - 0.457}{3} \right) = 80.18 \text{ kN}$$

Shear reinforcement are not required if  $V_{ED} \leq V_{Rd}$ ,

$$k = 1 + \sqrt{200/d}$$

$$k = 1 + \sqrt{200/457} = 1.66 \leq 2.0 \text{ ok}$$

$$A_{s1} = n * \pi * d_{main}^2$$

$$A_s = 1529.16 \text{ mm}^2$$

$$\rho_1 = \frac{A_{s1}}{b_w d} = \frac{1529.16}{250 * 457} = 0.0134 \leq 0.02$$

Take 0.0134

$$\sigma_{cp} = N_{ED} / A_c$$

$$\gamma_c = 1$$

$$C_{Rd,c} = 0.18 / \gamma_c = .18 / 1.0 = .18$$

$$v_{min} = 0.035 k^{3/2} f_{ck}^{1/2} = 0.035 * 1.66^{3/2} * 20^{0.5} = 0.335$$

$$k_1 = 0.15$$

$$V_{Rd,c} = \left[ C_{Rd,c} k (100 \rho_1 f_{ck})^{1/3} + k_1 \sigma_{cp} \right] b_w d$$

$$V_{Rd,c} = \left[ 0.18 * 1.66 (100 * .0134 * 20)^{1/3} + 1.5 * 0 \right] 250 * 457 = 115421.78 \text{ N}$$

$$\geq .335 * 250 * 457 = 38273.75 \text{ N Ok}$$

Check if the section is large enough or not

$$V_{Rd,max} = \alpha_{cw} b_w z v_1 f_{ck} / 1.5 * (\cot \theta + \tan \theta)$$

$$\alpha_{cw} = 1 \quad v_1 = 0.6 * (1 - \frac{f_{ck}}{250}) = 0.6 * (1 - \frac{20}{250}) = 0.552$$

$$z = 0.9 * 457 = 411.3 \text{ mm}$$

$$V_{Rd,max} = .54 * b_w d \frac{(1 - \frac{f_{ck}}{250})}{(\cot \theta + \tan \theta)} f_{ck}$$

$$V_{Rd,max} = .54 * 250 * 457 \frac{(1 - \frac{20}{250})}{(\cot \theta + \tan \theta)} * 20 = \frac{1135188}{(\cot \theta + \tan \theta)}$$

$$V_{Rd,max}(21.8^\circ) = \frac{11351188}{\cot(21.8)^\circ + \tan(21.8)^\circ} = 391444.137$$

$$V_{Rd,max}(45^\circ) = \frac{11351188}{\cot(45)^\circ + \tan(45)^\circ} = 567594N$$

$$V_{Rd,max} = \max \begin{cases} V_{Rd,max}(21.8^\circ) \\ V_{Rd,max}(45)^\circ \end{cases} = \max \begin{cases} 39144.137 \\ 567594 \end{cases} = 567594N$$

$$V_{Ed} = 80.13 \leq V_{Rd,max} = 567.594kN \text{ ok}$$

Determine the angle theta

$$V_{Ed} = V_{Rd,max} = 0.5 \sin 2\theta * 0.54 * b_w d (1 - f_{ck} / 250)$$

$$80130.00 = V_{Rd,max} = 0.5 \sin 2\theta * 0.54 * 250 * 457 * (1 - 20 / 250) = 28379.7 \sin 2\theta$$

$$\sin 2\theta = 80130.00 / 28379.7 = .282$$

$$\theta = 4.2^\circ \leq 21.8^\circ \text{ not ok}$$

So take 21.8

$$V_{Rd,max} = V_{Rd,max}(21.8^\circ) = 39144.137N$$

$$V_{Rd,max}(21.8^\circ) = \frac{11351188}{\cot(21.8)^\circ + \tan(21.8)^\circ} = 391444.137$$

Determine the angle  $\theta$

$$V_{ED} = V_{Rd,max} = 0.5 \sin 2\theta * 0.54 * b_w * d (1 - f_{ck} / 250)$$

$$\theta = 21.8$$

The maximum spacing between bars should not exceed

$$S_{max} = 0.75d \leq 600$$

$$S_{max} = 0.75 * 457 \leq 600$$

$$S_{max} = 342.75 \leq 600, \text{ ok}$$

Compute the stirrup spacing required to resist the shear force.

$$\frac{A_{sw}}{S} = \frac{V_{Ed}}{0.9df_{yk} \cot \theta} = \frac{80130}{.09 * 457 * 300 * 2.5} \geq \frac{0.08 * \sqrt{f_{ck}} * b_w}{f_{yk}} = \frac{0.08 * \sqrt{20} * 250}{300}$$

$$.26 \geq 0.298$$

$$\text{So } \frac{A_{sw}}{S} = 0.298$$

$$S = 100.48 / .298 = 337.02$$

$$S = \min \begin{cases} 337.02 \\ 342.75 \end{cases} = 337.02$$

Take the spacing to be 330mm

The total shear strength of the beam will be:

$$V_{Rd} = V_{Rd,s} = \frac{A_{sw}}{S} z f_{yd} \cot \theta$$

$$V_{Rd} = V_{Rd,s} = \frac{100.48}{330} * 0.9 * 457 * 300 * 2.5 = 93.99 \text{ kN}$$

**Case two :- Lightly reinforced** simply supported reinforced concrete beam subjected to concentrated loading at the center of the beam.

The critical shear section is at  $d$  distance from the support.

Using 25mm concrete cover and Ø8 for shear reinforcement, the structural depth can be calculated as

$$d = D - \phi / 2 - \phi_{stirrup} - cover$$

$$d = 300 - 25 - 8 - 8 = 259 \text{ mm}$$

$$V_{ED} = 40 * (2 - .2 - .259) = 30.82$$

$$V_{ED} = 40 * \left( \frac{2 - .2 - .259}{2} \right) = 30.82$$

Shear reinforcement are not required if  $V_{ED} \leq V_{Rd}$ ,

$$k = 1 + \sqrt{200 / d}$$

$$k = 1 + \sqrt{200 / 259} = 1.88 \leq 2.0 \text{ ok}$$

$$A_{s1} = n * \pi * d_{main}^2 = 3 * 3.14 * 10^2 = 942 \text{ mm}^2$$

$$\rho_1 = \frac{A_{s1}}{b_w d} = \frac{942}{250 * 259} = 0.015 \leq 0.02$$

$$\sigma_{cp} = N_{ED} / A_c$$

$$\gamma_c = 1$$

$$C_{Rd,c} = 0.18 / \gamma_c = .18 / 1.0 = .18$$

$$v_{min} = 0.035 k^{3/2} f_{ck}^{1/2} = 0.035 * 1.88^{3/2} * 20^{0.5} = 0.404$$

$$k_1 = 0.15$$

$$V_{Rd,c} = \left[ C_{Rd,c} k (100 \rho_1 f_{ck})^{1/3} + k_1 \sigma_{cp} \right] b_w d$$

$$V_{Rd,c} = \left[ 0.18 * 1.88 (100 * .014 * 20)^{1/3} + 1.5 * 0 \right] 200 * 259 = 57844.92N$$

$$\geq .404 * 200 * 259 = 20927.2N \text{ Ok}$$

Check if the section is large enough or not

$$V_{Rd,max} = \alpha_{cw} b_w z v_1 f_{ck} / 1.5 * (\cot \theta + \tan \theta)$$

$$\alpha_{cw} = 1$$

$$v_1 = 0.6 * \left( 1 - \frac{f_{ck}}{250} \right) = 0.6 * \left( 1 - \frac{20}{250} \right) = 0.552$$

$$V_{Rd,max} = .54 * b_w d \frac{\left( 1 - \frac{f_{ck}}{250} \right)}{(\cot \theta + \tan \theta)} f_{ck}$$

$$V_{Rd,max} = .54 * 250 * 259 \frac{\left( 1 - \frac{20}{250} \right)}{(\cot \theta + \tan \theta)} * 20 = \frac{643356}{(\cot \theta + \tan \theta)}$$

$$V_{Rd,max} (21.8^\circ) = \frac{514684.8}{\cot(21.8)^\circ + \tan(21.8)^\circ} = 176026.66N$$

$$V_{Rd,max} (45^\circ) = \frac{514684.8}{\cot(45)^\circ + \tan(45)^\circ} = 255355.12N$$

$$V_{Rd,max} = \max \begin{cases} V_{Rd,max} (21.8^\circ) \\ V_{Rd,max} (45)^\circ \end{cases} = \max \begin{cases} 176026.66 \\ 255355.12 \end{cases} = 255355.12N$$

$$V_{Ed} = 30.52 \leq V_{Rd,max} = 255.36kN \text{ ok}$$

Determine the angle theta

$$V_{Ed} = V_{Rd,max} = 0.5 \sin 2\theta * 0.54 * b_w d (1 - f_{ck} / 250)$$

$$30560.00 = V_{Rd,max} = 0.5 \sin 2\theta * 0.54 * 250 * 259 (1 - 20 / 250) = 12867.12 \sin 2\theta$$

$$\sin 2\theta = 30560 / 12867.12 = 2.38$$

$$\theta = 3.47^\circ \leq 21.8^\circ \text{ not ok}$$

So take  $\theta=21.8$

$$V_{Rd,max} = V_{Rd,max} (21.8^\circ) = 176026.66N$$

The maximum spacing between bars should not exceed

$$S_{max} = 0.75d \leq 600$$

$$S_{max} = 0.75 * 259 \leq 600$$

$$S_{max} = 194.75 \leq 600 \text{ ok}$$

Compute the stirrup spacing required to resist the shear force.

$$\frac{A_{sw}}{S} = \frac{V_{Ed}}{0.9d f_{yk} \cot \theta}$$

$$\frac{A_{sw}}{S} = \frac{V_{Ed}}{0.9d f_{yk} \cot \theta} \geq 0.08 * \frac{\sqrt{f_{ck}} * b}{f_{yk}}$$

$$\frac{A_{sw}}{S} = .175 \geq .239 = .239$$

$$\frac{A_{sw}}{S} = .175 \geq .239 = .239$$

$$S = \min \begin{cases} 192.75 \\ 421 \end{cases} = 190mm$$

The total shear strength of the beam will be

$$V_{Rd} = V_{Rd,s} = \frac{A_{sw}}{S} z f_{yd} \cot \theta$$

$$V_{Rd} = V_{Rd,s} = \frac{100.48}{190} * 0.9 * 259 * 300 * 2.5 = 91.80kN$$

**Case three:-** Cantilever reinforced concrete beam subjected to uniform loading.

The critical shear section is at  $d$  distance from the support.

Using 25mm concrete cover and Ø8 for shear reinforcement

$$d = D - \phi / 2 - \phi_{stirrup} - cover$$

$$d = 350 - 25 - 8 - 10 = 307mm$$

$$V_{ED} = 200 * \left( \frac{2 - .2 - .307}{2} \right) = 149.3kN$$

Shear reinforcement are not required if  $V_{ED} \leq V_{Rd}$ .

$$k = 1 + \sqrt{200/d}$$

$$k = 1 + \sqrt{200/307} = 1.81 \leq 2.0 \text{ ok}$$

$$A_{s1} = 1808mm^2$$

$$\rho_1 = \frac{A_{s1}}{b_w d} = \frac{1808}{250 * 307} = 0.023 \leq 0.02$$

Take 0.02

$$\sigma_{cp} = N_{ED} / A_c$$

$$\gamma_c = 1$$

$$C_{Rd,c} = 0.18 / \gamma_c = .18 / 1.0 = .18$$

$$v_{min} = 0.035k^{3/2} f_{ck}^{1/2} = 0.035 * 1.81^{3/2} * 20^{0.5} = 0.381$$

$$k_1 = 0.15$$

$$V_{Rd,c} = \left[ C_{Rd,c} k (100 \rho_1 f_{ck})^{1/3} + k_1 \sigma_{cp} \right] b_w d$$

$$V_{Rd,c} = \left[ 0.18 * 1.81 (100 * .02 * 20)^{1/3} + 1.5 * 0 \right] 250 * 457 = 85516N$$

$$\geq .335 * 250 * 307 = 29241.75N \text{ Ok}$$

**Check if the section is large enough or not**

$$V_{Rd,max} = \alpha_{cw} b_w z v_1 f_{ck} / 1.5 * (\cot \theta + \tan \theta)$$

$$\alpha_{cw} = 1$$

$$v_1 = 0.6 * (1 - \frac{f_{ck}}{250}) = 0.6 * (1 - \frac{20}{250}) = 0.552$$

$$z = 0.9 * 307 = 276.3mm$$

$$V_{Rd,max} = .54 * b_w d \frac{(1 - \frac{f_{ck}}{250})}{(\cot \theta + \tan \theta)} f_{ck}$$

$$V_{Rd,max} = .54 * 250 * 307 \frac{(1 - \frac{20}{250})}{(\cot \theta + \tan \theta)} * 20$$

$$V_{Rd,max} (21.8^\circ) = 175307.59N$$

$$V_{Rd,max} (45^\circ) = 254196N$$

$$V_{Rd,max} = \max \begin{cases} V_{Rd,max} (21.8^\circ) \\ V_{Rd,max} (45^\circ) \end{cases} = \max \begin{cases} 175307.59 \\ 254196 \end{cases} = 254196N$$

$$V_{Ed} = 149.3 \leq V_{Rd,max} = 254.19kN \text{ ok}$$

Determine the angle theta

$$V_{Ed} = V_{Rd,max} = 0.5 \sin 2\theta * 0.54 * b_w d (1 - f_{ck} / 250)$$

$$149300 = V_{Rd,max} = 0.5 \sin 2\theta * 0.54 * 250 * 457 (1 - 20 / 250) * 20$$

$$\sin 2\theta = .39$$

$$\theta = 11.52^\circ \leq 21.8^\circ, \text{ not ok}$$

So take 21.8

$$V_{Rd,max} = V_{Rd,max} (21.8^\circ) = 39144.137N$$



The maximum spacing between bars should not exceeded

$$S_{\max} = 0.75d \leq 600$$

$$= 0.75 * 307 \leq 600$$

$$S_{\max} = 230.25 \leq 600 \text{ ok}$$

Compute the stirrup spacing required to resist the shear force

$$\frac{A_{sw}}{S} = \frac{V_{Ed}}{0.9df_{yk} \cot \theta}$$

$$\frac{2 * 3.14 * 4 * 4}{S} = \frac{149.3 * 1000}{.9 * 307 * 300 * 2.5} = .72$$

$$S = 100.48 / .72 = 139.56 \text{ mm}$$

Take the spacing to be 130mm

The total shear strength of the beam will be:

$$V_{Rd} = V_{Rd,s} = \frac{A_{sw}}{S} z f_{yd} \cot \theta$$

$$V_{Rd} = V_{Rd,s} = \frac{100.48}{130} * 0.9 * 307 * 300 * 2.5 = 160.27 \text{ kN}$$

**Table 4-1 Summary of shear results of Euro code shear design procedure**

Item	Case 1	Case 2	Case 3	Case 4	Case 5
vrdc (kN)	102.21	57.84	85.38	96.06	115.23
Vrd,max,21.8 (kN)	391.27	176.03	262.84	305.65	366.78
Vrd,max,45 (kN)	567.59	255.36	381.29	443.39	532.07
Vrd,max (kN)	567.59	255.36	381.29	443.39	532.07
Thetha, cal	4.04	3.31	9.12	4.72	7.66
Smax (mm)	342.75	192.75	381.29	267.75	267.75
Asw/S (mm <sup>2</sup> /mm)	0.3	0.24	0.58	0.3	0.58
S,cal (mm)	337.02	421.28	174.64	333.52	172.46
provide phi c/c (mm)	330	190	170	260	170
Vrd (kN)	93.99	91.8	122.56	93.19	142.52

#### 4.2.2 Design Procedure Using ACI Code

The critical shear section is located  $d$  distance from the support.

Using 25 mm concrete cover and  $\phi$  8 for shear reinforcement.

**Case one:- lightly reinforced simply supported beam subjected to uniform loading**

$$d = D - \phi / 2 - \phi_{stirrup} - cover$$

$$V_u = V_{\max} \left( \frac{l/2 - d - columnwidth}{l} \right)$$

$$V_u = 102 * \left( \frac{3 - .457 - .2}{3} \right) = 80.13 \text{ kN}$$

$$V_n = \frac{V_u}{\phi}, \text{ where } \phi \text{ accounts for the type of aggregate used.}$$

Shear reinforcement is not required if,  $V_n \leq V_c / 2$

$$V_c = \frac{\lambda \sqrt{f'_c} b_w d}{6}$$

$$V_c = \frac{1\sqrt{20} * 250 * 457}{6} = 85156.92 \text{ N}$$

Check whether shear reinforcement is required or not?

$$V_n = 80130 \geq V_c / 2 = 42578.46 \text{ ok}$$

So shear reinforcement is required.

Check whether the section is large enough or not?

$$V_{s,\max} = \frac{2}{3} (\sqrt{f'_c} b_w d)$$

$$V_{s,\max} = \frac{2}{3} (\sqrt{20} * 250 * 457) = 340627.69 \text{ N}$$

$$\left(\frac{V_u}{\phi}\right)_{\max} = V_c + V_{s,\max}$$

$$\left(\frac{V_u}{\phi}\right)_{\max} = 85156.92 + 340627.69 = 425784.61N$$

$$\left(\frac{V_u}{\phi}\right)_{\max} = 85156.92 + 340627.69 = 425784.61N \geq V_n \text{ ok}$$

Hence the section is large enough.

Using  $\emptyset 8$  stirrup,

$$A_v = 2 * \pi * \phi^2 / 4 = 100.48 \text{ mm}^2$$

Calculate of maximum spacing of shear reinforcements.

$$S_{\max} \leq \begin{cases} \begin{cases} 0.5d \\ 600 \end{cases}, \text{ if } \rightarrow V_s \leq \sqrt{f_c'} b_w d \\ \begin{cases} 0.25d \\ 300 \end{cases}, \text{ if } \rightarrow V_s > \frac{1}{3} \sqrt{f_c'} b_w d \end{cases}$$

$$\frac{1}{3} \sqrt{f_c'} b_w d = \frac{1}{3} \sqrt{20} * 250 * 457 = 170.31kN$$

$$V_s = V_n - V_c = 85.156 - 80.13 = 5.03kN \leq 170.31$$

$$S_{\max} = \begin{cases} 0.5 * 457 = 228.5 \\ 600 \end{cases} = 228.5mm$$

Maximum spacing based on minimum shear reinforcement.

$$A_{v,\min} = \frac{1}{16} \sqrt{f_c'} \frac{b_w S}{f_{yt}} \geq \frac{1}{3} \frac{b_w S}{f_{yt}}$$

$$\frac{1}{16} \sqrt{20} = .28 < \frac{1}{3}$$

$$S_{\max} = \frac{3 * A_v f_{yt}}{b_w} = \frac{3 * 100.48 * 300}{250} = 551mm$$

Compare  $S_{\max}$  based on depth and minimum

$$S_{\max} = \min \begin{cases} 228.5 \text{ mm} \\ 551 \text{ mm} \end{cases} = 228.5 \text{ mm}$$

Determine the shear reinforcement spacing require to resist the applied shear force.

$$S = \frac{A_v f_y d}{\frac{V_u}{\phi} - V_c} = \frac{100.48 * 300 * 457}{5.03 * 1000} = 2738.8 \text{ mm}$$

$$S_{\max} = \min \begin{cases} 228.5 \text{ mm} \\ 2738 \text{ mm} \end{cases} = 228.5 \text{ mm}$$

So take the spacing to be 220mm

The total shear strength of the beam for the calculated spacing will be:

$$V_c + \frac{A_v f_y d}{S} = 85156 + \frac{100.48 * 300 * 457}{220} = 147.77 \text{ kN}$$

**Case two:- Lightly reinforced simply supported beam subjected to concentrated loading**

$$d = 300 - 25 - 8 - 8 = 259 \text{ mm}$$

$$V_u = V_{\max} \left( \frac{l - d - \text{columnwidth}}{l} \right) = 55.52 \text{ kN}$$

$$V_n = \frac{V_u}{\phi}, \text{ where } \phi \text{ accounts for the type of aggregate used.}$$

Shear reinforcement is not required if,  $V_n \leq V_c / 2$

$$V_c = \frac{\lambda \sqrt{f'_c} b_w d}{6}$$

$$V_c = \frac{1 \sqrt{20} * 250 * 259}{6} = 48261.80 \text{ N}$$

Check whether shear reinforcement is required or not?

$$V_n = 55520 \geq V_c / 2 = 24130.90N, \text{ ok}$$

So shear reinforcement is required.

Check whether the section is large enough or not?

$$V_{s,\max} = \frac{2}{3}(\sqrt{f_c'} b_w d)$$

$$V_{s,\max} = \frac{2}{3}(\sqrt{20} * 250 * 259) = 193047.02 \text{ N}$$

$$\left(\frac{V_u}{\phi}\right)_{\max} = V_c + V_{s,\max}$$

$$\left(\frac{V_u}{\phi}\right)_{\max} = 48261 + 193047.02 = 241308.20N$$

$$\left(\frac{V_u}{\phi}\right)_{\max} = 241308.20N \geq V_n = 55520 \text{ ok}$$

Hence the section is large enough

Using  $\phi$  8 stirrup,

$$A_v = 2 * \pi * \phi^2 / 4 = 100.48 \text{ mm}^2$$

Calculate of maximum spacing of shear reinforcements.

$$S_{\max} \leq \begin{cases} \begin{cases} 0.5d \\ 600 \end{cases}, \text{ if } \rightarrow V_s \leq \sqrt{f_c'} b_w d \\ \begin{cases} 0.25d \\ 300 \end{cases}, \text{ if } \rightarrow V_s > \frac{1}{3} \sqrt{f_c'} b_w d \end{cases}$$

$$\frac{1}{3} \sqrt{f_c'} b_w d = \frac{1}{3} \sqrt{20} * 250 * 259 = 96523.60kN$$

$$V_s = V_n - V_c = 55.52 - 48.26 = 7.26kN \leq 96.52$$

$$S_{\max} = \begin{cases} 0.5 * 259 = 129.5 \\ 600 \end{cases} = 129.50mm$$

Maximum spacing based on minimum shear reinforcement.

$$A_{v,\min} = \frac{1}{16} \sqrt{f_c} \frac{b_w S}{f_{yt}} \geq \frac{1}{3} \frac{b_w S}{f_{yt}}$$

$$\frac{1}{16} \sqrt{20} = .28 < \frac{1}{3}$$

$$S_{\max} = \frac{3 * A_v f_{yt}}{b_w} = \frac{3 * 100.48 * 300}{250} = 551mm$$

Compare  $S_{\max}$  based on depth and minimum spacing

$$S_{\max} = \min \begin{cases} 129.5 \text{ mm} \\ 551 \text{ mm} \end{cases} = 129.5mm$$

Determine the shear reinforcement spacing require to resist the applied shear force.

$$S = \frac{A_v f_{yt} d}{\frac{V_u - V_c}{\phi}} = \frac{100.48 * 300 * 259}{7.2 * 1000} = 942.91mm$$

$$s=120mm$$

The total shear strength of the beam for the calculated spacing will be:

$$V_c + \frac{A_v f_{yt} d}{S} = 48261 + \frac{100.48 * 260.87 * 259}{120} = 106.43kN$$

**Case three:- Heavily reinforced cantilever beam subjected to uniform loading**

$$d = 350 - 25 - 8 - 10 = 307mm$$

$$V_u = V_{\max} \left( \frac{l - d - \text{columnwidth}}{l} \right) = 149.3kN$$

$$V_n = \frac{V_u}{\phi}, \text{ where } \phi \text{ accounts for the type of aggregate used.}$$

Shear reinforcement is not required if,  $V_n \leq V_c / 2$

$$V_c = \frac{\lambda \sqrt{f'_c} b_w d}{6}$$

$$V_c = \frac{1\sqrt{20} * 250 * 307}{6} = 57206.07 N$$

Check whether shear reinforcement is required or not?

$$V_n = 149.3 \geq V_c / 2 = 28.603 kN, \text{ ok}$$

So shear reinforcement is required.

Check whether the section is large enough or not

$$V_{s,max} = \frac{2}{3} (\sqrt{f'_c} b_w d)$$

$$V_{s,max} = \frac{2}{3} (\sqrt{20} * 250 * 307) = 227824.30 N$$

$$\left(\frac{V_u}{\phi}\right)_{max} = V_c + V_{s,max}$$

$$\left(\frac{V_u}{\phi}\right)_{max} = 57206.07 + 227824.30 = 285010.37 N$$

$$\left(\frac{V_u}{\phi}\right)_{max} = 285010.37 N \geq V_n = 149300 N \text{ ok}$$

Hence the section is large enough

Using  $\emptyset 8$  stirrup,

$$A_v = 2 * \pi * \phi^2 / 4 = 100.48 \text{ mm}^2$$

Calculate of maximum spacing of shear reinforcements.

$$S_{\max} \leq \begin{cases} 0.5d \\ 600 \end{cases}, \text{if } \rightarrow V_s \leq \sqrt{f_c'} b_w d$$

$$\begin{cases} 0.25d \\ 300 \end{cases}, \text{if } \rightarrow V_s > \frac{1}{3} \sqrt{f_c'} b_w d$$

$$\frac{1}{3} \sqrt{f_c'} b_w d = \frac{1}{3} \sqrt{20} * 250 * 307 = 114.412kN$$

$$V_s = 149.30 - 57.206 = 92.09kN \leq 96.52$$

$$S_{\max} = \begin{cases} 0.5 * 307 = 153.5 \\ 600 \end{cases} = 153.50mm$$

Maximum spacing based on minimum shear reinforcement.

$$A_{v,\min} = \frac{1}{16} \sqrt{f_c'} \frac{b_w S}{f_{yt}} \geq \frac{1}{3} \frac{b_w S}{f_{yt}}$$

$$\frac{1}{16} \sqrt{20} = .28 < \frac{1}{3}$$

$$S_{\max} = \frac{3 * A_v f_{yt}}{b_w} = \frac{3 * 100.48 * 300}{250} = 551mm$$

Compare  $S_{\max}$  based on depth and minimum spacing

$$S_{\max} = \min \begin{cases} 153.5 \text{ mm} \\ 551 \text{ mm} \end{cases} = 153.5mm$$

Determine the shear reinforcement spacing require to resist the applied shear force.

$$S = \frac{A_v f_{yt} d}{\frac{V_u - V_c}{\phi}} = \frac{100.48 * 300 * 307}{92.09 * 1000} = 87.38mm$$

$$s=80mm$$

The total shear strength of the beam for the calculated spacing will be:

$$V_c + \frac{A_v f_{yt} d}{S} = 57206.07 + \frac{100.48 * 260.87 * 307}{80 * 1000} = 157.80kN$$



**Table 4-2 Summary of the shear design results of ACI shear design procedure**

Item	Case 1	Case 2	Case 3	Case 4	Case 5
Vc(Kn)	85.156922	383.11	572.06	66.52	79.83
Vs,max(N)	340627.69	153.24	228.82	266.09	319.93
Vu,max(N)	425784.61	191.56	286.03	332.62	399.14
S,max(mm)	228.5	128.5	153.5	178.5	178.5
Av,min(mm <sup>2</sup> /m)	0.28	0.22	0.28	0.28	0.33
S,cal(mm)	2766.53	390	149.04	1757	177.4
S, rovided(mm)	220	120	140	170	170
Vrd(kN)	147.77	102.87	123.31	129.83	143.13

**Table 4-3 Summary of shear design results**

Case	B(mm)	H(mm)	Shear Capacity(kN)	
			ACI	Euro
1	250	500	147.77	93.99
2	200	300	106.43	91.8
3	250	350	123.31	122.56
4	250	400	128.93	93.19
5	300	400	143.13	142.52

#### 4.2.3 Shear Strength Calculation Using MCFT

Shear capacity of the beam sections subjected to different loading was calculated by the c# program. Inputs were provided and the program was run and shear values were calculated. The inputs and the results are shown in the table below.

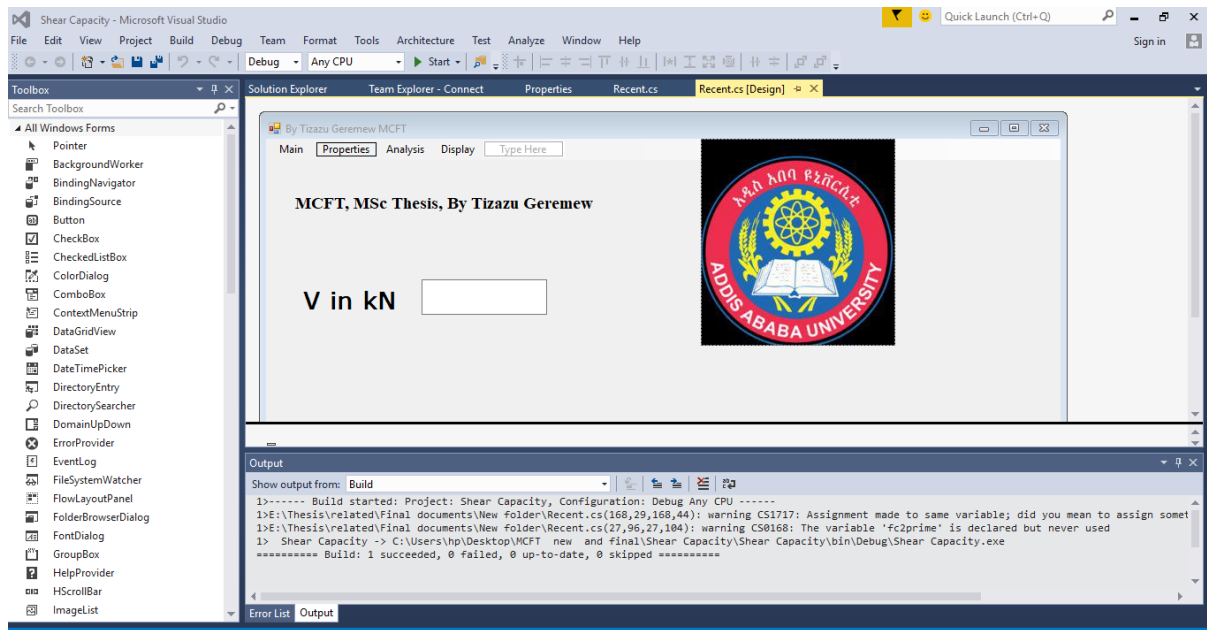


Figure 4.3 Main window showing menu strips

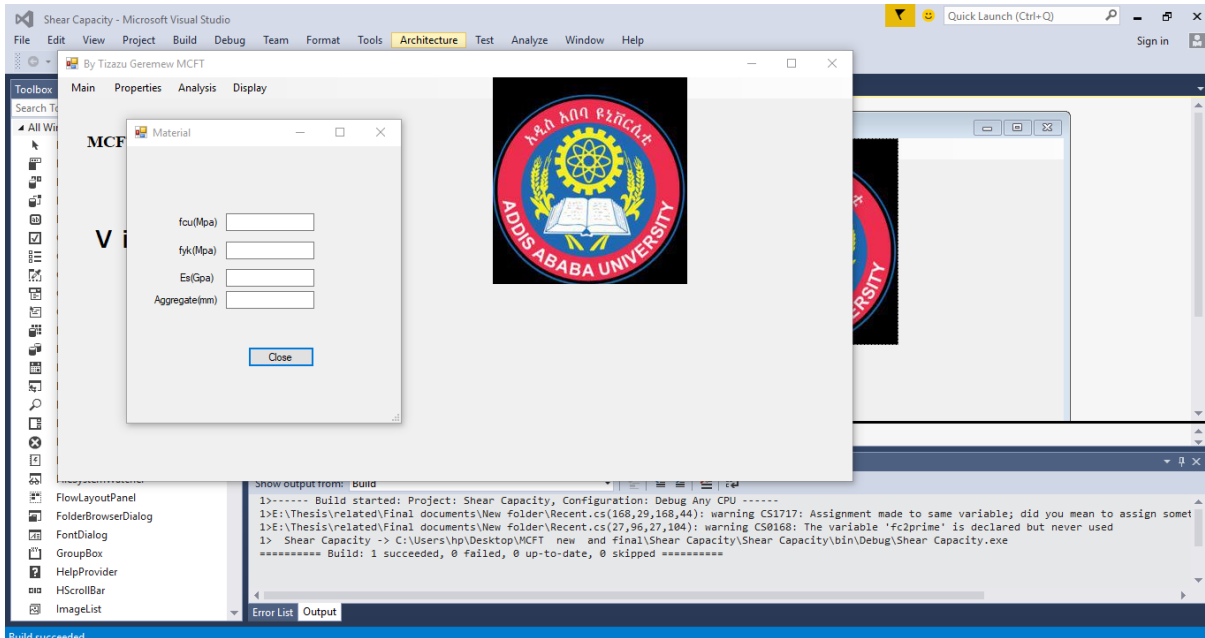


Figure 4.4 Main window showing material properties

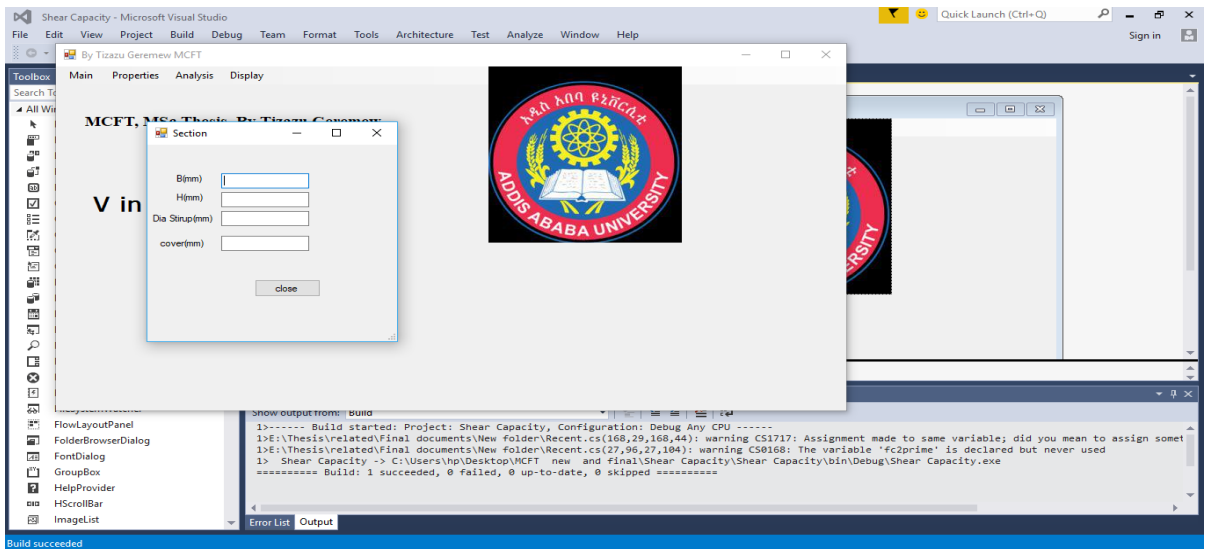
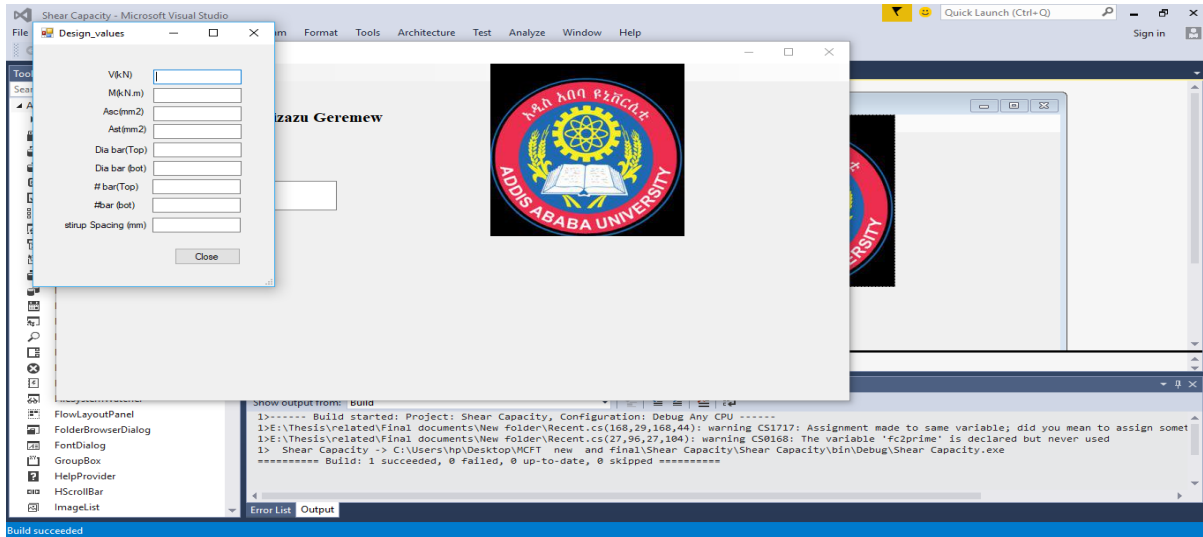


Figure 4.5 Main window showing section properties



**Figure 4.6** Main window showing design inputs

## Chapter 5 RESULT AND DISCUSSION

**Table 5-1 Comparison of shear capacity of sections according to Euro Code, ACI and MCFT**

<b>Approach</b>	<b>Case one</b>	<b>Case two</b>	<b>Case three</b>
EURO CODE	79.68	26.8	86.23
MCFT,Eurocode	331.96	259.9	195.07
% of increment	76.00	89.69	55.80
ACI	147.77	106.43	157.8
MCFT, ACI	361.94	318.8	267.92
% of increment	59.17	66.62	41.10

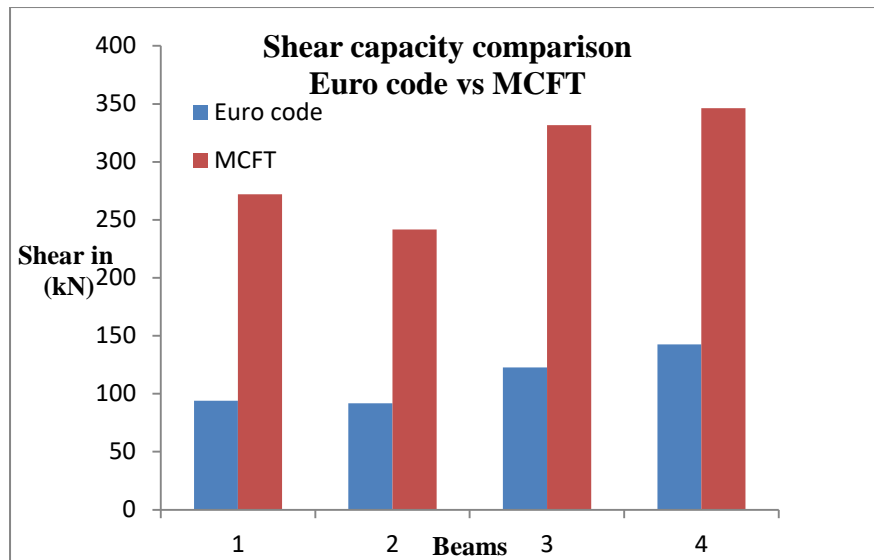


**Figure 5.1 Comparison of MCFT and Euro code**

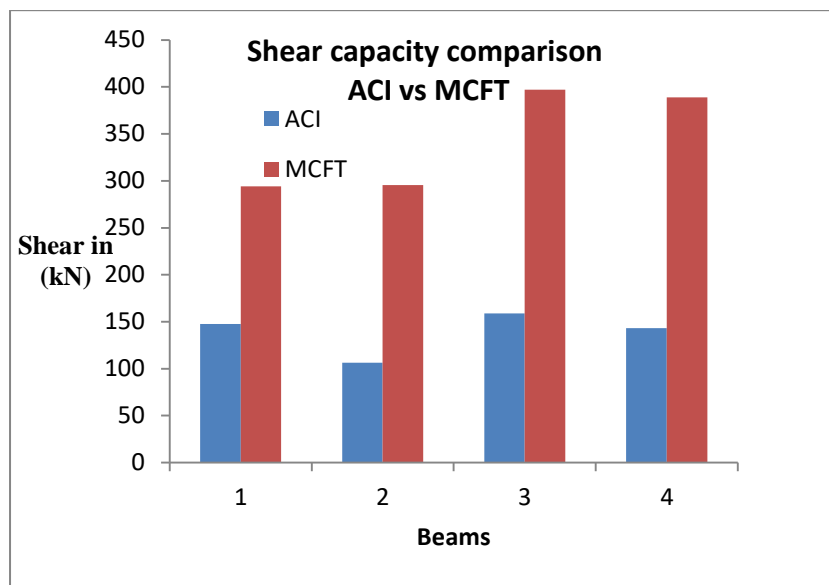


**Figure 5.2 Comparison of ACI and MCFT**

It is very clear that Euro code is more conservative design approach in estimating shear design of reinforced concrete beams. That is why the list values are obtained in the analysis. Whereas, ACI code gives better estimation as compared to Euro code and this is because the concrete is assumed to contribute for shear in shear design procedure.

As it is shown in Figure 5.1 and Figure 5.2 above the shear capacity of beam sections obtained by modified compression field theory is greater than those of the Euro code values and the ACI code values. This mainly because of the assumption that, in modified compression field theory concrete between cracks can contribute to the shear capacity of a

section. The differences are relatively more significant between MCFT and Euro code. That is why this theory should get more attention by researchers.

## **Chapter 6 CONCLUSIONS AND RECOMMENDATIONS**

### **6.1 Conclusions**

As it is shown in the Figure 5.1 and Figure 5.2 the shear capacity of beam sections obtained by modified compression field theory is greater than those of the Euro code values and the ACI code values. This is mainly because of the assumption that, in modified compression field theory concrete between cracks can contribute to the shear capacity of a section. That is why this theory should get more attention by researchers.

In addition to this, the shear capacities of the beam sections estimated by the ACI code are also higher than that of the Euro code. Obviously this is because of the difference in the assumptions in the two codes. In Euro code it is assumed that the shear resistance of the section is due to the stirrups in designing for shear, where as in ACI code the concrete contribution is also considered in addition to the the stirrups.

In general shear design using modified compression field theory is more reliable than the available design codes. Not only it predicts the shear capacity accurately but also tells the failure criteria. So, further researches can be done on shear design and capacity checking so that our understanding of shear will be improved.

### **6.2 Recommendations**

The main aim of this thesis was to get a tool to solve the complex mathematical problem in modified compression field theory. Due to this little attention was given to additional concepts in this theory. For the sake of completeness future researches can be done in the following areas.

- Capturing the effects of factors that affect shear resistance of a reinforced concrete structures.
- Since modified compression field theory does not consider the effect of shear slip in the design process, it should be considered.



- Also for deep beams modified compression field theory will not be preferable instead disturbed stress field theory should be applied. So the response of deep beams can be studied by adopting such computer programs. (Bentz, 2000)
- Size effect can also be another area of further investigation in relation to MCFT.
- Since modified compression field theory can predict the failure mode of reinforced concrete structures subjected to shear new design procedures can be proposed and incorporated in to codes.

## REFERENCE

- Belarbi, A. &. (1994). Constitutive Laws of Concrete in Tension and Reinforcing Bars Stiffened by Concrete. *ACI Structural Journal*, 1-20.
- Bentz, E. C. (2000). *Sectional Analysis of Reinforced Concrete Members*. Toronto: National Library of Canada.
- Chan, T. (2008). *Role of Force Resultant Interaction on Fiber Reinforced Concrete*. Florida: University of Central Florida.
- Collins, M. M. (1991). Prestressed Concrete Structures. *Prentice Hall*,, 338-411.
- Esfandiari, A. (2009). *Shear Strength of Structural Concrete*. Vancouver: The University of British Columbia.
- Ghannoum, W. M. (1998). *Size Effect on Shear Resistance of Reinforced Concrete Beams*. Montreal: McGill University.
- Gregory P. Pasley. (December 1990). *Shear Strength of Continuous Beams*. Kansas: University of Kansas.
- Güner, Serhan. (2008). *Performance Assesment of Shear Critical beams*. Toronto: University of Toronto.
- Ingham, R. R. (2012). *Assessment of Shear Stress limits in New Zealand Design Standards for Highstrength Concrete Bridge Beams*. Auckland: NZ Transport Agency research report.
- J. A. Ramirez etal. (1999). *Recent Approaches to Shear Design of Structural Concrete*. ACI-ASCE Committee.
- Kraczla, M. J. ( 2016). *Analytical and Numerical Analysis of the Shear Tension Critical*. Delft: Delft University of Technology.
- Krings, H. (2014). *Shear Failure of Reinforced Concrete Beams with Steel Fibre Reinforcement*. Eindhoven: Eindhoven University of Technology.

- Kyoung-Kyu Choi; Woo-Chang Sim; Jong-Chan Kim; and Hong-Gun Park. (2014). Maximum Shear Strength of Slender RC Beams with. *Journal of Structural Engineering*, 1-9.
- M Al-Ani, R. R. (2012). *Assessment of Shear Stress Limits in*. Auckland: NZ Transport Agency.
- MacGregor, J. G., and Wight, J. K. (2005). *Reinforced Concrete Mechanics and Design*. Pearson Education, Inc.
- María, G.-M. L. ( 2012). A Simpler Compression Field Theory for Structural Concrete. *Studies And Researches*, 7-9.
- Marti, P. (1985). Basic Tools of Beam Design. *ACI journal, Proceedings, Vol. 82, No.1*, 46-59.
- Michael P. Collins, Denis Mitchell, Perry Adebar and Frank J. Vecchio;. ((January-February 1996, )“). A General Shear Design Method. *ACI Structural journal, Proceedings*., Title No.93-S5.
- S.Pillai, Devdas Menon and S.Pillai. (2009). *Reinforced Concrete Design”, 3rd Edition*., Chicago: Tata McGraw-Hill Education Pvt. Ltd.
- Sas, G. (2011). *FRP Shear Strengthening of Reinforced Concrete Structures*. Luleå: Universitetstryckeriet.
- Shuaib H. Ahmad, S. S. (2012). Shear Predictions of Eurocode EC2. *American Journal of Civil Engineering and Architecture*, 43-46.
- Tsegaye, S. (2016). *Assessing Code Based Shear Prediction Values of Reinforced Concrete Beams*. Addis Ababa: AAU.

## APPENDIX A:

```
using System;

using System.Collections.Generic;

using System.ComponentModel;

using System.Data;

using System.Drawing;

using System.Linq;

using System.Text;

using System.Threading.Tasks;

using System.Windows.Forms;

namespace Shear_Capacity

{

    public partial class Form1 : Form

    {

        public Material CopyMaterial=new Material();

        public Section copysection = new Section();

        public Design_values copydesignvalues = new Design_values();

        public e1_Vs_Vci_graph copyGraph = new e1_Vs_Vci_graph();

        public Form1()

        {

            InitializeComponent();

            private void runAnalysisToolStripMenuItem_Click(object sender, EventArgs e)

            {

                Double

                Moment=0,N=0,eyd,fs_tension,fs_compression,fsycr,G,F,fc1,eo,beta,fc2max,fc2,fc2prime,gammaxy,fyd,e2,ey,f

                sy,kk,Agg,fcr,ecr,fc1,AA,BB,CC, st, cx,cy,sx,sy,smx,smy,top_No_of_bar,bot_No_of_bar, fxi =

                0,exi,etop,ebot,phi, I,V,M,q,Es, fcu, fyk, phistirup, diatop, diabot, Ast, Asc, Ec, b, d, h, cover, dprime;

                Agg = Convert.ToDouble(CopyMaterial.agregate.Text);

                double teta, s_teta,w, Vci_max, fc1max, vci=0, DD, delta_fc1;

                st = Convert.ToDouble(copydesignvalues.Spacing_st.Text);
```

```

top_No_of_bar = Convert.ToDouble(copydesignvalues.topbar.Text);
bot_No_of_bar = Convert.ToDouble(copydesignvalues.botbar.Text);

Es = Convert.ToDouble(CopyMaterial.Steel_Modulus.Text);
fcu = Convert.ToDouble(CopyMaterial.conc_grade.Text);
fyk = Convert.ToDouble(CopyMaterial.steel_Grade.Text);
  phistirup = Convert.ToDouble(copysection.phi_stirup.Text);
diatop = Convert.ToDouble(copydesignvalues.Topbar_dia.Text);
diabot = Convert.ToDouble(copydesignvalues.botombar_dia.Text);
Ast = Convert.ToDouble(copydesignvalues.Tension_steel.Text);
Asc = Convert.ToDouble(copydesignvalues.comp_steel.Text);
double fcprime = 0.8 * fcu;
double Ecprime = 3320 * Math.Pow(fcprime, 0.5)+6900;
Ec = Ecprime;
b = Convert.ToDouble(copysection.width.Text);
h = Convert.ToDouble(copysection.depth.Text);
cover = Convert.ToDouble(copysection.clear_cover.Text);
d = h - cover - phistirup - diabot / 2;
dprime = cover + phistirup + diatop / 2;
fyd = fyk / 1.15;
eyd = fyd / (1000*Es);
V = Convert.ToDouble(copydesignvalues.acting_shear.Text);
M = Convert.ToDouble(copydesignvalues.acting_Moment.Text);
q = V*1000 / h;
eo = -0.002;
double bw = 3.5 * b;
for(double e1=0.0015;e1<=0.002;e1+=0.000001)
{
for (double x = dprime; x <= d; x += (d - dprime) / 10)
{
for (double y = h / 40; y <= h; y += h / 20)

```

```

{
I = x * x * x * b / 12 + (Es*1000 / Ec) * Asc * (x - dprime) * (x - dprime) + (Es*1000 / Ec) * Ast * (d - x) * (d -
x);

phi = M * 1000000*x / (Ec * I);

etop = x * phi;

ebot = (d - x) * phi;

exi = etop * (x - y) / x;

fxi =fxi + exi * Ec * h * b / 20000;

// cracking properties
cx = d - x - diabot / 2;

cy = b / 2 - cover - phistirup;

sx = (b - bot_No_of_bar * diabot - 2 * (cover + phistirup)) / (bot_No_of_bar - 1);

sy = Convert.ToDouble(copydesignvalues.Spacing_st.Text);

smx = 2* (cx + sx / 10) + 0.25 * 0.4 * Math.Max(diabot, diatop) / ((Asc + Ast) / (b * h));

smy = 2 * (cy + sy / 10) + 0.25 * 0.4 * phistirup / (3.14 * phistirup * phistirup * 0.25 / (st * b));

//cracking stress of concrete

fcr = 0.33 * Convert.ToDouble(Math.Pow(0.8 * Convert.ToDouble(fcu), 0.5));

ecr = fcr / Ec;

//steel stresses

//A)top bar stress
if (ebot < eyd)
{
fs_tension = ebot * Es*1000;
}
else
{
fs_tension = fyd;
}

//B) compression bar stress
if (etop < eyd)

```

```

{
fs_compression = -etop * Es*1000;
}
else
{
fs_compression = -fyd;
}
//Principal tensile stress
if (e1<ecr)
{
fc1 = e1 * Ec;
}
else
{
fc1 = fcr / (1 + Math.Pow(500 * (e1), 0.5));
}
// Calculation of inclination of cracks (Theta)
CC=-Es*1000*e1-fc1 / (3.14 * phistirup * phistirup * 0.25 / (st * b));
BB = V*1000 / (b * h * 3.14 * phistirup * phistirup * 0.25 / (st * b));
if(Es * (e1 - exi)>0)
{
AA = Es*1000* (e1 - exi);
}
else
{
AA = 0.000000000001;
}
double AAA = Convert.ToDouble(AA);
double BBB = Convert.ToDouble(BB);
double CCC = Convert.ToDouble(CC);

```

```

double x1 =Math.Atan((-BBB + Math.Pow(BBB * BBB - 4 * AAA * CCC, 0.5)) / (2 * AAA));
double x2 = Math.Atan((-BBB - Math.Pow(BBB * BBB - 4 * AAA * CCC, 0.5)) / (2 * AAA));
teta = Math.Max(x1, x2);
if(teta==0)
{
continue;
}
s_teta = 1 / (Math.Sin(teta) / (double)smx + Math.Cos(teta) / (double)smy);
// Crack width calculation
w = (double)e1 * s_teta;
Vci_max = Math.Pow(0.8 * Convert.ToDouble(fcu), 0.5) / (0.31 + 24 * w / (double)Agg + 16);
kk = 1.64 - 1 / Math.Tan(teta);
ey = e1 - (e1 - exi) * (Math.Pow(Convert.ToDouble((Math.Tan(Convert.ToDouble(teta)))), 2));
e2 = exi - (e1 - exi) * (Math.Pow(Convert.ToDouble((Math.Tan(Convert.ToDouble(teta)))), 2));
gammaxy= 2*(e1 - exi) * (Math.Pow(Convert.ToDouble((Math.Tan(Convert.ToDouble(teta)))), 2));
fyd = fyk / 1.15;
fsy = ey * Es*1000;
fc1max = Vci_max * (0.18 + 0.3 * (double)kk * (double)kk * ((Math.Tan(Convert.ToDouble(teta)))) + (3.14 *
(double)phistirup * (double)phistirup*((double)fyd-(double)fsy) / 4);
fcprime = fc1 - (V/(b * h)) *
(Convert.ToDecimal(Math.Tan(Convert.ToDouble(teta)))+1m/((Convert.ToDecimal(Math.Tan(Convert.ToDo
uble(teta))));
    beta = 0.8 + 170 * e1;
fc2max = fcu / (0.8 * beta);
if (-fc2max >= -fcu / 0.8)
{
fc2max = fcu / 0.8;
}
else
{
fc2max = fc2max;
}

```



```

}

fc2 = fc2max * ((2 * e2 / eo) - (Math.Pow(Convert.ToDouble(e2 / eo), 2)));

delta_fc1 = fc1 - (3.14 * phistirup * phistirup * (fyd - fsy) / 4);

if (delta_fc1 <= 0)

{

vci+= 0.0001;

fci = 0.0001;

}

else

DD = delta_fc1 / ((Math.Tan(Convert.ToDouble(teta))))-0.18*Vci_max;

if (DD <= 0)

{

fci = 0.0000001;

vci+= delta_fc1 / ((Math.Tan(Convert.ToDouble(teta))));

}

else

{

G = 0.82 / Vci_max;

F = 1 / ((Math.Tan(Convert.ToDouble(teta)))) - 1.64;

fci=(-F-(Math.Pow((Math.Pow(Convert.ToDouble(F),2)-Convert.ToDouble((4*G*DD))),0.5))/ (2 * G));

vci+= (fc1 + delta_fc1) / ((Math.Tan(Convert.ToDouble(teta))));

}

}

fsycr = fsy + (fc1 + fci - vci * (Math.Tan(Convert.ToDouble(teta)))) / (3.14 * phistirup * phistirup / (4 * b * st));

// Failure criteria

if (fc1 > fc1max)

{

MessageBox.Show("slipping on the crack governs");

}

if (fc2 > fc2max)

```

```

{
MessageBox.Show("crushing governs");
}

if (fsycr > fyd)
{
MessageBox.Show(" The reinforcement is Not capable of transmitting the loads across the cracks");
}

N = ( fxi + fs_compression * Asc + fs_tension * Ast)/1000;
double Mcc = (exi / 1000 * Ec * h * (b / 20) * y) / 1000000;
double Mcs = fs_compression * Asc * dprime / 1000000;
double Mst = (fs_tension * Ast * d)/ 1000000;

Moment = Moment + Mcc + Mcs + Mst;

Asc = 0m; Ast = 0m;

if (N < 10)
{
if (N > -10)
{
if (Moment - M < 500)
{
if (Moment - M > -500)
{
if ( (teta == 0 || teta == double.NaN))
{
}
}
else
{
x = 3 * h;
}
else
{

```

```

}
}
else
{
}
}
}
}
Moment = 0;
}
}
}
textBox1.Text = Math.Round(vci * bw * h / 2000000000000, 2).ToString();
if (fc1 > fc1max)
{
MessageBox.Show("slipping on the crack governs");
}
if (fc2 > fc2max)
{
MessageBox.Show("crushing governs");
}
if (fsycr > fyd)
{
MessageBox.Show(" The reinforcement is Not capable of transmitting the loads across the cracks");
}
MessageBox.Show("Analysis complete");
}
private void materialToolStripMenuItem1_Click(object sender, EventArgs e)
{
CopyMaterial.ShowDialog();
}

```

```

}

private void sectionToolStripMenuItem_Click(object sender, EventArgs e)
{
copysection.ShowDialog();
}

private void designValuesToolStripMenuItem_Click(object sender, EventArgs e)
{
copydesignvalues.ShowDialog();
}

private void e1VsVciGraphToolStripMenuItem_Click(object sender, EventArgs e)
{
copyGraph.ShowDialog();
}

private void listBox2_SelectedIndexChanged(object sender, EventArgs e)
{
}

private void listBox1_SelectedIndexChanged(object sender, EventArgs e)
{
}

private void label1_Click(object sender, EventArgs e)
{
}

private void analysisToolStripMenuItem_Click(object sender, EventArgs e)
{
}
}
}
}

```